

Late Cenozoic deformation and uplift of the western flank of the Altiplano: Evidence from the depositional, tectonic, and geomorphologic evolution and shallow seismic activity (northern Chile at 19°30'S)

Marcelo Farías,^{1,2,3} Reynaldo Charrier,¹ Diana Comte,² Joseph Martinod,³ and Gérard Hérail⁴

Received 13 April 2004; revised 4 February 2005; accepted 11 March 2005; published 1 July 2005.

[1] We analyze the west vergent thrust system (WTS) along the western flank of the Altiplano in northern Chile (18°S–21°S). In our study area (19°20'S–19°50'S), the WTS consists of three thrust propagation monocline folds (flexures) developing growth strata. The relative uplift accommodated by the flexures is rapid between 26 and 8 Ma (0.1 mm/yr), diminishing to 0.02 mm/yr after 8 Ma. Approximately 2000 m of relative surface uplift was accommodated by the flexures since the late Oligocene. Sedimentological and geomorphological analysis shows that westward tilting of the forearc occurred after 10 Ma, coeval with the shifting of deformation from the Altiplano to the sub-Andean zone, where the underthrusting of the Brazilian Craton would have resulted in crustal thickening, surface uplift in the orogen, and westward ductile subcrustal flow. Forearc tilting is accommodated by east vergent thrusts (ETS) issued from the Benioff zone beneath the Central Depression emerging into the Western Cordillera, contributing 500–1400 m of surface uplift. The WTS connects the ETS in the brittle-ductile crustal transition (~25 km depth), continuing farther east as the Altiplano low-velocity zone, configuring the western Altiplano as a crustal-scale fault bend fold. Forearc tilting would be caused by westward ductile flow in the lower crust pushing the rigid forearc in the ETS. Meanwhile, between 19°S and 21°S, the WTS accommodates dextral strike slip, and ~3 km of N-S shortening occurred in the Coastal Cordillera. Transcurrence and strain partitioning are probably the result of slight plate convergence obliquity, strong coupling within the interplate zone, westward continental concavity, and high elevation opposing

horizontal contraction. **Citation:** Farías, M., R. Charrier, D. Comte, J. Martinod, and G. Hérail (2005), Late Cenozoic deformation and uplift of the western flank of the Altiplano: Evidence from the depositional, tectonic, and geomorphologic evolution and shallow seismic activity (northern Chile at 19°30'S), *Tectonics*, 24, TC4001, doi:10.1029/2004TC001667.

1. Introduction

[2] The western margin of South America is one of the largest and most active plate boundary zones. Here, the oceanic Nazca plate (or formerly Farallon plate) subducts beneath the South American continent at a rate of 84 mm/yr [DeMets *et al.*, 1994]. The Andes are located along this border (Figure 1) and can be subdivided into the northern, central, and southern Andes according to its geological features [Gansser, 1973]. The curved portion of the central Andes in northern Chile, southern Peru, and Bolivia is the broadest part of the mountain belt (Figure 1). This segment of the range includes the Altiplano-Puna, which is the highest plateau formed on a noncollisional margin (~4 km high) [Isacks, 1988], and the second in the world after the Tibetan plateau.

[3] The origin of this mountain belt is attributed to contractional strain related to almost uninterrupted subduction since the Jurassic along the western margin of South America [Baby *et al.*, 1997; Coira *et al.*, 1982; Jordan *et al.*, 1983; Kay and Abbruzzi, 1996; Kay *et al.*, 1991, 1999; Mpodozis and Ramos, 1989; Ramos, 1988; Sempere *et al.*, 1990]. However, the major present-day features of the central Andes were formed during the Cenozoic, and particularly during the last 30 Myr [e.g., Allmendinger *et al.*, 1997; Isacks, 1988; Lamb *et al.*, 1997; Rutland, 1971; Sempere *et al.*, 1990]. Since then and after major plate reorganization, the Nazca and South American plates increased their velocity of relative convergence, which became almost orthogonal to the Chilean margin [Pardo-Casas and Molnar, 1987; Somoza, 1998].

[4] The present-day crustal thickness (60–80 km) and surface elevation of the Altiplano is mainly considered to be a consequence of large crustal shortening [Allmendinger *et al.*, 1997; Beck and Zandt, 2002; Haschke and Günther, 2003; Husson and Sempere, 2003; Isacks, 1988; Lamb and Hoke, 1997; Lamb *et al.*, 1997; McQuarrie, 2002; McQuarrie and DeCelles, 2001; Reutter *et al.*, 1988;

¹Departamento de Geología, Universidad de Chile, Santiago, Chile.

²Departamento de Geofísica, Universidad de Chile, Santiago, Chile.

³Laboratoire des Mécanismes et Transferts en Géologie, Université Paul Sabatier, Toulouse, France.

⁴Institut de Recherche pour le Développement, Laboratoire des Mécanismes et Transferts en Géologie, Toulouse, France.

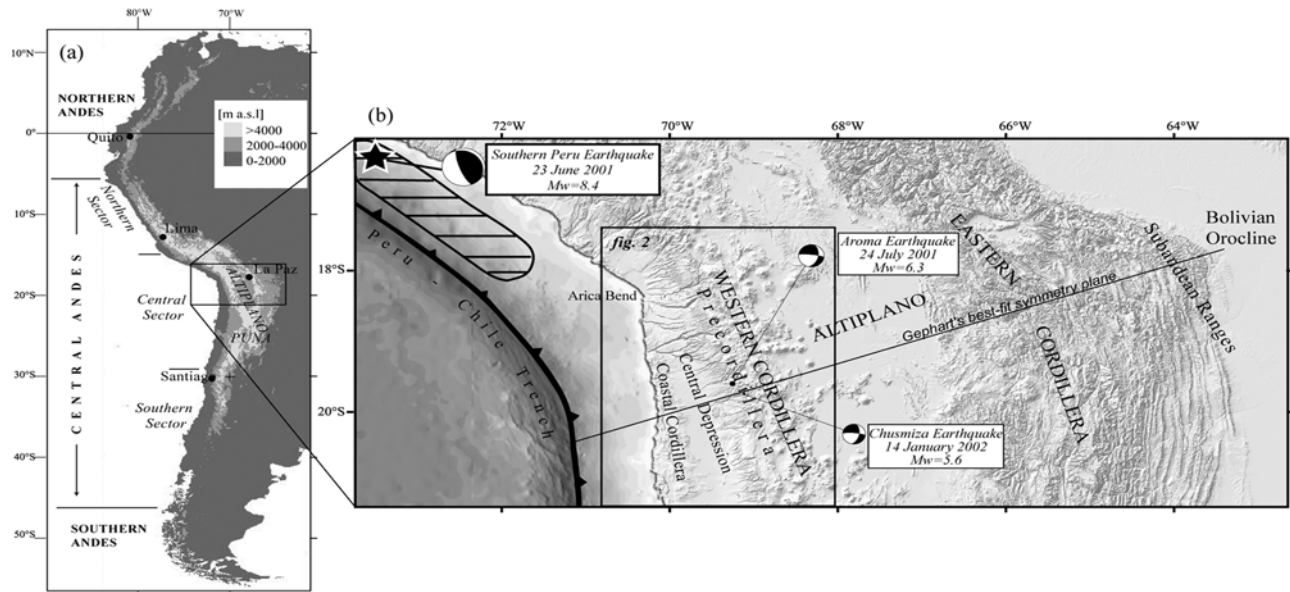


Figure 1. (a) Western margin of South America, showing the subdivision of the Andes into northern, central and southern [Gansser, 1973]. (b) Topography of the central Andes Altiplano of northern Chile, southern Peru, and Bolivia based on the SRTM 90 m digital elevation model (<http://seamless.usgs.gov/>) and the NOAA 2 min bathymetric database (<http://www.noaa.gov/>). The main morphostructural features of this region are the Peru-Chile trench where the oceanic Nazca plate is overridden by South America; the Coastal Cordillera; the Central Depression; the Precordillera; the Western Cordillera; the Altiplano basin; the Eastern Cordillera; and the sub-Andean Ranges. The hatched area is the rupture zone of the southern Peru interplate earthquake (23 June 2001).

Roeder, 1988; Schmitz, 1994; Sheffels, 1990]. However, some discrepancy exists between the observed tectonic shortening and the amount of material needed to explain the entire crustal thickness [Allmendinger *et al.*, 1997; Husson and Sempere, 2003; Kley and Monaldi, 1998; Kley *et al.*, 1997; Lamb *et al.*, 1997; McQuarrie, 2002; Schmitz, 1994]. In addition, geophysical and petrological studies suggest that other processes would have been involved in crustal thickening and plateau surrection, such as magmatic addition [Gill, 1981; Hoke *et al.*, 1994; Kono *et al.*, 1989; Weaver and Tarney, 1984], lithospheric thinning and removal of the subcrustal lithosphere [Beck and Zandt, 2002; Isacks, 1988; Lamb *et al.*, 1997; Whitman *et al.*, 1996], underplating of material removed from the forearc by subduction erosion [e.g., Baby *et al.*, 1997; Schmitz, 1994], and ductile mass transfers within the lower crust [Beck and Zandt, 2002; Gerbault *et al.*, 2002; Husson and Sempere, 2003; Kley and Monaldi, 1998].

[5] Most tectonic studies in the central Andes Altiplano have been focused on the back arc region, mainly in the Eastern Cordillera and sub-Andean Ranges, where a large upper crustal shortening (200–350 km) has been accommodated since Cretaceous times by the predominantly east vergent Andean fold-and-thrust belt. Nevertheless, in most studies referred to the plateau development, the tectonic activity accommodated along the monocline-shaped western flank of the Altiplano has been almost neglected, simply because the observed Neogene deformation is much less than the shortening on the eastern flank.

[6] For over a decade, several studies have been performed in northern Chile [Charrier *et al.*, 1999, 2000, 2002; García, 1996, 2002; García *et al.*, 1996, 1999, 2002; Muñoz and Charrier, 1996; Muñoz and Sepúlveda, 1992; Pinto *et al.*, 2004; Parraguez, 1998; Victor *et al.*, 2004] that show the existence of an almost continuous system of west vergent contractional structures in the monocline along a north-to-south distance of >300 km (Figure 2), although it presents changes in its geometry, orientation, amount of deformation, and expression on the Cenozoic cover. Muñoz and Charrier [1996] grouped these structures into the west vergent thrust system (WTS). This system continues farther north in southernmost Peru for >100 km along the Sierra Huaylillas (Figure 2). The great length of this structural system suggests that the WTS is a major tectonic feature in this part of the Andes, and seems to have been an essential structural element that accommodated deformation on this side of the Altiplano. However, the shortening and uplift related to the activity of the WTS has not yet been well documented. This has generated controversies about the real contribution of the WTS to the uplift of the western Altiplano (see discussion by García and Hérail [2001] and Wörner and Seyfried [2001]).

[7] In addition to the geological studies, considerable crustal shallow seismic activity has been reported along the forearc in northern Chile and southern Peru [Comte *et al.*, 2001, 2002, 2003a, 2003b; David *et al.*, 2002; Haessler *et al.*, 2000]. The shallow Aroma earthquake ($M_w = 6.3$, 24 July 2001, Figures 1 and 2) is the major expression of the

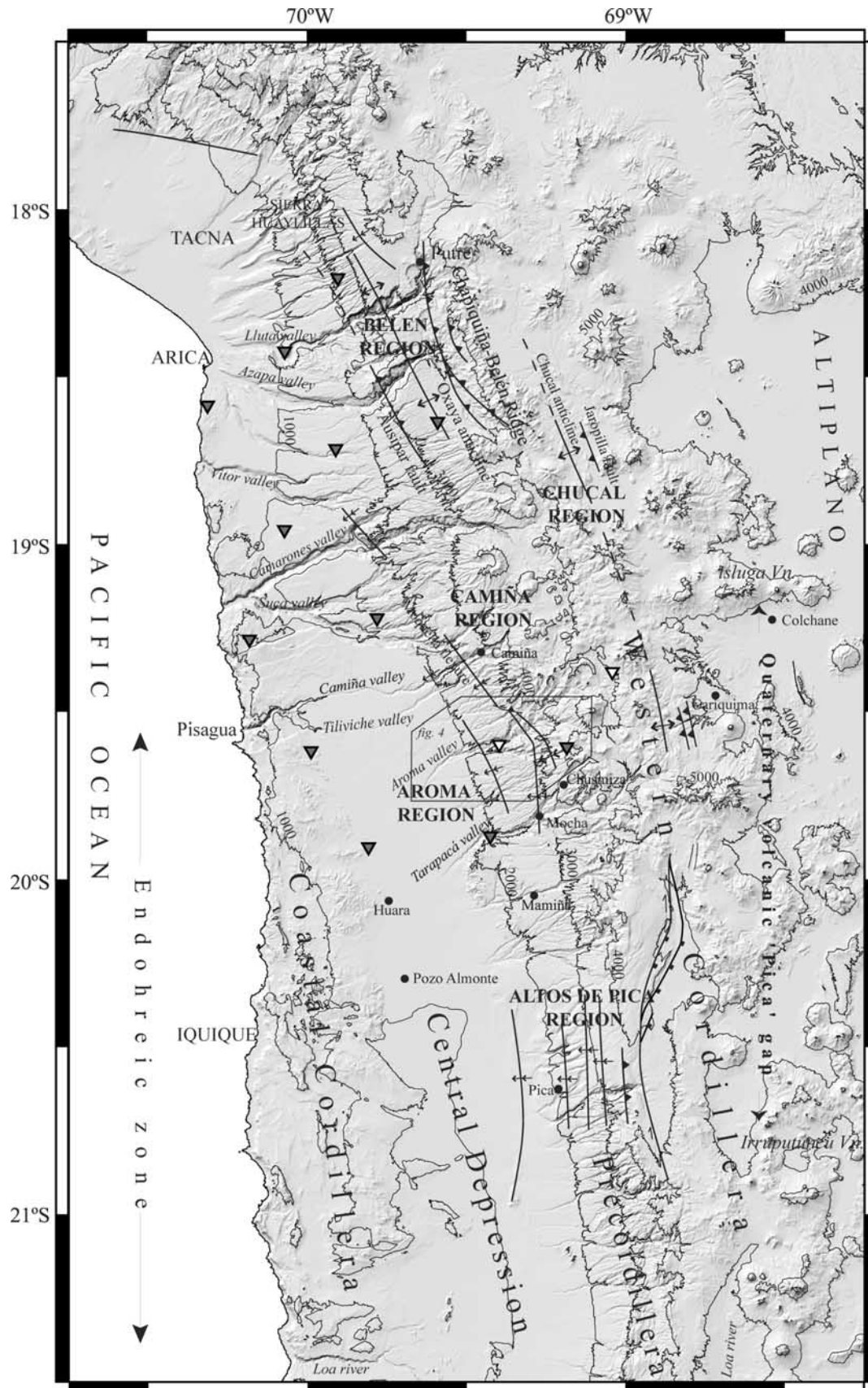


Figure 2

seismic activity on the Chilean forearc, which occurred one month after the interplate southern Peru earthquake ($M_w = 8.4$, 23 June 2001, Figure 1). Crustal seismicity bordering the western side of the Altiplano suggests that tectonic activity is still important in this region, and that it is probably associated with deformation along the WTS.

[8] This paper focuses on the tectonic evolution of the western slope of the Altiplano in the region adjacent to the Aroma valley ($19^{\circ}20'S$ – $19^{\circ}50'S$) between the Central Depression and the Western Cordillera, where the late Cenozoic cover is exceptionally well exposed. In this area, the WTS consists of several west dipping monocline folds developing growth strata on the Cenozoic cover. This allows us to determine relative uplift and constrain the age of activity. Our work is complemented by stratigraphic and geomorphologic observations, and with the seismic record of the Aroma earthquake aftershocks. On the basis of our findings in the studied area, in conjunction with regional correlation, we propose a model for the late Cenozoic development of the western flank of the Altiplano in northern Chile and the contribution of the WTS to this evolution.

2. Geological Background

[9] Along the western flank of the Altiplano in northern Chile, four main morphotectonic units are recognized in the onshore forearc of the Tarapacá region (Figure 2). The westernmost unit, the Coastal Cordillera (or Coastal Ranges) has a smooth relief up to 1200 m in altitude bordering the Pacific Ocean. The Central Depression (or Longitudinal Valley) is a N-S trending elongated basin, endorheic between the Tiliviche valley and Loa river (Figure 2), with a mean altitude of 1000 m. The Precordillera (1500–3600 m high) is a gentle west sloping surface crossed by W-E trending narrow deep valleys. The Western Cordillera has an irregular topography (3800–4700 m above sea level (asl)), crowned by Neogene to present-day stratovolcanoes (5000–6900 m asl). The Central Depression, the Precordillera, and the Western Cordillera form the “monocline-shaped” western flank of the Altiplano [Isacks, 1988].

[10] Along the western margin of the high plateau in northern Chile and southern Peru, a N-S to NNW-SSE trending, high-angle west vergent thrust system is developed (Figure 2) [García, 1996; García et al., 1996; Muñoz and Charrier, 1996; Muñoz and Sepúlveda, 1992]. At the latitude of Arica ($18^{\circ}30'S$), this system is formed by the Copaquilla-Belén, Cerro Lagunas-Belén-Tignámar, and Copaquilla-Tignámar faults, and the Ausipar fault located farther west at the boundary between the Precordillera and the Central Depression. This last fault caused the development of the Oxaya Anticline at its rear (Figure 2) [García, 1996; García et al., 1996, 1999]. In addition, several low-amplitude folds deform the Cenozoic cover between the

Central Depression and Precordillera [García, 2002]. Between the Camarones valley and the Altos de Pica region ($19^{\circ}10'S$ – $21^{\circ}S$) (Figure 2) a west vergent fault propagation fold system is developed along the Precordillera [Farías et al., 2002; Pinto et al., 2004; Victor et al., 2004] corresponding to the southward continuation of the WTS observed at the latitude of Arica.

[11] An east vergent structural system composed of the Jaropilla fault and the Chucal anticline [Riquelme, 1998; Riquelme and Hérail, 1997; Charrier et al., 2002], is located on the SE side of the Chapiquiña-Belén ridge at the Western Cordillera of Arica ($\sim 19^{\circ}S$, Figure 2). According to Charrier et al. [2002] this system was mainly active before 10 Ma.

[12] The development of the west and east vergent contractional structures was associated with complex processes of erosion and deposition, which generated widely distributed syntectonic sediments, volcanoclastic and volcanic deposits along the Western Cordillera, the Precordillera and the Central Depression, unconformably overlying a Precambrian?–early Paleozoic to Paleocene substratum.

[13] In the Precordillera and Central Depression of northern Chile, the late Cenozoic cover corresponds to a thick sequence of clastic deposits and ignimbrites. In the Arica region (Figure 3) the series consists of the Oligocene alluvial-fluvial deposits of the Azapa Formation [Salas et al., 1966; Parraguez, 1998], the lower Miocene ignimbritic deposits of the Oxaya Formation [García, 1996; Montecinos, 1963] and the middle Miocene conglomerates of the El Diablo Formation [Parraguez, 1998; Tobar et al., 1968; Vögel and Vila, 1980]. To the south, along the Precordillera and Central Depression between the Suca valley ($\sim 19^{\circ}10'S$) and the Altos de Pica region ($\sim 21^{\circ}S$), the Oligo-Miocene series is named the Altos de Pica Formation [Galli, 1957, 1967; Galli and Dingman, 1962]. This formation corresponds to a thick sequence of ignimbrites and gravels, originally subdivided into five members by Galli and Dingman [1962] at the type locality. This formation can be correlated with the deposits known in the Arica region (Figure 3): the lower member (Member 1 of the Altos de Pica Formation [Galli and Dingman, 1962]) correlated with the Azapa Formation; the middle members (members 2, 3 and 4) correlated with the Oxaya Formation; and the upper member (Member 5) correlated with the El Diablo Formation. In conjunction, the Azapa, Oxaya and El Diablo Formation in the Arica region ($18^{\circ}15'S$ – $19^{\circ}S$), as well as their equivalent farther south (the Altos de Pica Formation) in the Iquique region ($19^{\circ}S$ – $21^{\circ}S$), constitute a great sedimentary and volcanic unit produced by a compensation to the Andean uplift, in a climatic environmental that favored piedmont formation by means of debris accumulation during Oligocene-Neogene times [Naranjo and Paskoff, 1985].

Figure 2. Shaded relief map based on SRTM 90 m DEM showing the main late Cenozoic structures of the western flank of the Altiplano in northern Chile (Tarapacá Region). Gray triangles correspond to the seismological stations of the permanent seismological and telemetrical network of northern Chile (RESISTE-ARICA), and the open triangles correspond to the temporal seismological stations deployed after the Aroma earthquake. The box indicates the study area (Aroma region) shown in Figure 4.

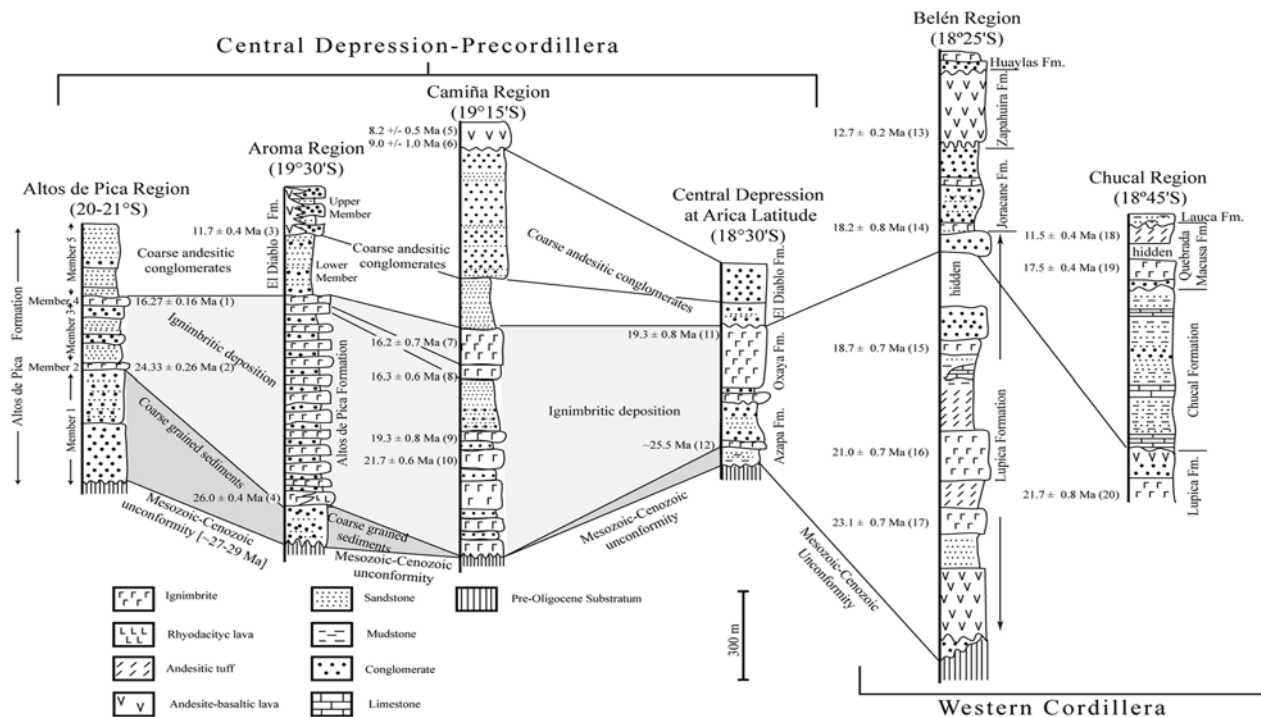


Figure 3. Simplified stratigraphic logs of the Cenozoic cover in the North Chilean forearc, based on the work by Pinto *et al.* [2004] (Camiña Region), Galli and Dingman [1962] and Victor *et al.* [2004] (Altos de Pica Region), Parraguez [1998] and García [2002] (Central Depression at Arica Latitude), García [1996, 2002] (Belén Region), Riquelme [1998] and Charrier *et al.* [2002] (Chucal Region), and this work (Aroma region) where new stratigraphic nomenclature is used (see section 3.2). The location of each zone is shown in Figure 2. Ages are detailed in Table 1.

[14] The Western Cordillera and eastern Precordillera have been dominated since middle-late Miocene by the activity of volcanic complexes (Figure 3). The series is represented by the Oligo-early Miocene volcanic Lupica Formation [García, 1996; Montecinos, 1963; Riquelme, 1998; Salas *et al.*, 1966], the middle Miocene syntectonic-conglomeratic Joracane Formation [García, 1996], the middle Miocene andesite-basaltic Zapahuira Formation [García, 1996], and the late Miocene-Pleistocene syntectonic sediments of the Huaylas Formation [García, 1996, 2002; Salas *et al.*, 1966; Viteri, 1979]. On the eastern side of the Western Cordillera, overlying a 21.7 ± 0.7 Ma white tuff level assigned to the Lupica Formation, the following units are present: the gently folded sedimentary series of the Chucal Formation [Charrier *et al.*, 2002; Riquelme, 1998], and the volcanic and sedimentary series of the Quebrada Macusa Formation [Charrier *et al.*, 2002; Riquelme, 1998]. To the top of the series lies the late Miocene-Pliocene fluvial and lacustrine Lauca Formation [Gaupp *et al.*, 1999; Kött *et al.*, 1996].

3. Geology of the Aroma Region

3.1. Pre-Oligocene Substratum

[15] In the following, we call substratum all the rocks older than the Oligocene, which were studied by Harambour

[1990]. The substratum crops out east of the Aroma flexure (see Figures 4 and 5).

[16] The Quebrada Aroma Formation (the oldest unit) is a 1000- to 1500-m-thick rhythmic sequence of metasandstones and metalutites. This unit exhibits metamorphism and ductile deformation, with some local development of mylonites adjacent to the hinge line of the Aroma flexure. Fossil rests (Chondites sp. tracks and microfossils) contained in the lower part of this formation suggest a late Paleozoic age, probably not older than the late Devonian [Harambour, 1990]. This formation is unconformably overlain by Mesozoic (lower Jurassic to lower Cretaceous) back arc deposits, which form a ~2000-m-thick succession of continental coarse volcanoclastics and ash tuffs, containing some marine layers in its lower portion [Harambour, 1990]. Harambour [1990] recognized two stages of tectonic development during the Mesozoic: a first stage dominated by extensional tectonics and subsidence from Sinemurian to lower Oxfordian times and a second stage characterized by basin inversion causing gentle folding and thrusting before deposition of the late Cenozoic series.

3.2. Synorogenic Clastics and Volcanics

[17] In the study region, the late Cenozoic cover has been grouped into the Altos de Pica Formation (APF), formerly defined by Galli and Dingman [1962] in the Altos de Pica

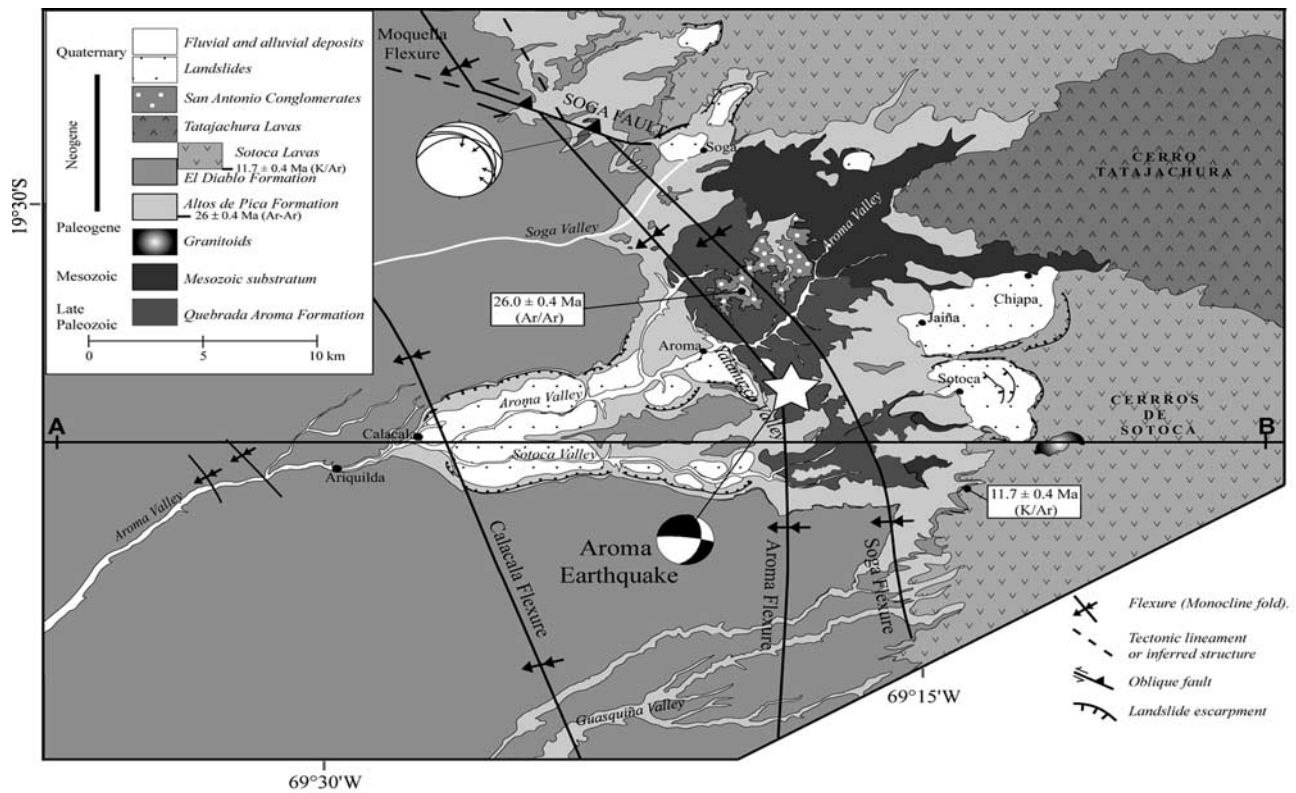


Figure 4. Geologic map of the study area.

region ($\sim 69^\circ\text{W}/\sim 20^\circ 30'\text{S}$). In this paper, we have assigned the upper member (Member 5) of the original definition of *Galli and Dingman* [1962] to the El Diablo Formation because of (1) its similarity with the clastic unit defined in the Central Depression at the Arica latitude and (2) the differences in lithological and environmental framework between that upper member and the underlying members of the former definition. Hereafter, we will refer to the four lower members of the former *Galli and Dingman*'s [1962] definition as the Altos de Pica Formation and to the Member 5 of the former definition as the El Diablo Formation.

3.2.1. Altos de Pica Formation

[18] This formation corresponds to an alternation of ignimbrites and continental volcanoclastic conglomerates and breccias with some interbedded sandstones and siltstones, with a mean thickness of 600 m. Because of lithological differences and correlation with other stratigraphic units of northern Chile, we subdivide the APF into a lower and upper member (see below). The APF overlies the pre-Oligocene substratum above a major unconformity. In the Tarapacá valley ($19^\circ 50'\text{S}$, Figure 2), this unconformity corresponds to an irregular paleorelief, which is almost

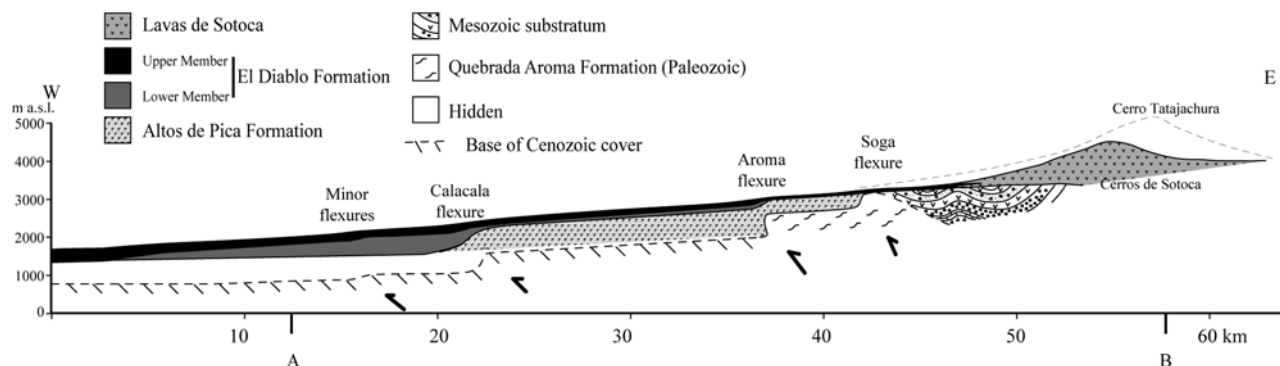


Figure 5. Cross section of the study area. Outcrops only are hatched. The contact between substratum and Cenozoic cover is estimated on the basis of the observed surface deformation. A-B section is displayed into the geologic map (Figure 4).

Table 1. Radiometric Ages for the Late Cenozoic Volcanic Deposits in the Western Flank of the Altiplano in Northern Chile

	Age, Ma	Method ^a	Location	Author
1	16.27 ± 0.16	Rb/Sr (Bt-Hbl)	20°13'S/68°69'W	<i>Victor et al.</i> [2004]
2	24.33 ± 0.26	Rb/Sr (Bt-Hbl)	20°29'S/69°21'W	<i>Victor et al.</i> [2004]
3	11.7 ± 0.4	K/Ar (WR)	19°38'S/69°13'W	this study
4	26.0 ± 0.4	Ar/Ar (Bt)	19°32'S/69°20'W	this study
5	8.2 ± 0.5	K/Ar (WR)	Pampa Tana	<i>Muñoz and Sepúlveda</i> [1992]
6	9.0 ± 1.0	K/Ar (WR)	19°20'S/69°33'W	<i>Naranjo and Paskoff</i> [1985]
7	16.2 ± 0.7	K/Ar (WR)	19°13'S/69°37'W	<i>Muñoz and Sepúlveda</i> [1992]
8	16.3 ± 0.6	K/Ar (Bt)	19°13'S/69°38'W	<i>Muñoz and Sepúlveda</i> [1992]
9	19.3 ± 0.8	K/Ar (Bt)	19°22'S/69°32'W	<i>Pinto</i> [1999]
10	21.7 ± 0.6	K/Ar (Bt)	19°22'S/69°32'W	<i>Naranjo and Paskoff</i> [1985]
11	19.3 ± 0.8	K/Ar (Bt)	18°46'S/69°49'W	<i>Parraguez</i> [1998]
12	25.4 ± 0.7	K/Ar (Bt)	18°56'S/69°31'W	<i>García</i> [2002]
	25.5 ± 0.8		19°01'S/69°56'W	
	25.6 ± 0.9		19°01'S/69°56'W	
13	12.7 ± 0.2	K/Ar (WR)	18°23'S/69°37'W	<i>García</i> [1996]
14	18.2 ± 0.8	K/Ar (WR)	18°29'S/69°32'W	<i>García</i> [1996]
15	18.7 ± 0.7	K/Ar (Bt)	18°45'S/69°17'W	<i>García</i> [2002]
16	21.0 ± 0.7	K/Ar (Bt)	18°42'S/69°13'W	<i>García</i> [2002]
17	23.1 ± 0.7	K/Ar (Bt)	18°29'S/69°31'W	<i>García</i> [1996]
18	11.5 ± 0.5	Ar/Ar (Pl)	18°43'S/69°06'W	<i>Wörner et al.</i> [2000]
19	17.5 ± 0.4	Ar/Ar (Bt)	18°44'S/69°10'W	<i>García</i> [2002]
20	21.7 ± 0.8	K/Ar (Bt)	18°42'S/69°13'W	<i>García</i> [2002]

^aMaterial dated WR, whole rock; Bt, biotite; Bt-Hbl, biotite-hornblend isochrone; Pl, plagioclase. Numbers in first column correspond to the ages shown in Figure 3.

completely filled by the lower member of the APF. Summits of this paleorelief are flat-shaped surfaces of approximately equal altitude. In contrast, west to the Aroma flexure in the Aroma and Sotoca valleys, the contact between the APF and the substratum is flat. There, the lower APF member is absent or has a reduced thickness. This flat-shaped unconformity suggests a pre-Oligocene pedimentation event (the “Choja Pediplain” of *Galli* [1967]), whereas paleovalleys excavated on this surface would represent a rejuvenation of the landscape, possibly coeval to the onset of accumulation of the lower member of the APF [*Fariás et al.*, 2003; *Galli*, 1967]. Similar features in the unconformity between the late Cenozoic deposits and the substratum have been reported in southernmost Peru in the Altos de Camilaca surface [*Tosdal et al.*, 1984].

[19] The lower member of the APF (in the sense of this study) consists of polymictic conglomerates, breccias, and minor immature sandstones. Clasts have compositions similar to the underlying substratum, suggesting the beginning of denudation, and probably marking the onset of uplift of the western flank of the Altiplano [*Dingman and Galli*, 1965; *Mortimer and Saric*, 1975; *Naranjo and Paskoff*, 1985; *Victor et al.*, 2004]. Its thickness is variable: from the Soga to the Sotoca valleys, east of the Aroma flexure, it is <8 m thick, whereas west of this flexure, its thickness increases to ~100 m; along the Tarapacá valley the thickness varies between 10 and 200 m, depending on the shape and depth of the paleovalleys.

[20] The upper member (in the sense of this study, members 2, 3, and 4 of the former definition of *Galli and Dingman* [1962]) forms the main part of the APF in the study area. This homogeneous member consists of at least 12 layers of ignimbrites interbedded with thin, often coarse sedimentary layers. Ignimbrites are welded ash tuffs, rich in

quartz and biotite, with minor sanidine and pyroxene. Shards and rhyolitic fragments are contained in the matrix, which diminish to the west, away from the volcanic centers. The two upper ignimbrites of the series have a wide regional extension in the Tarapacá region. The lower one (Tarapacá ignimbrite [*Muñoz and Sepúlveda*, 1992; *Pinto et al.*, 2004]) is a dark vitrophyre overlain by the Nama ignimbrite [*Pinto et al.*, 2004]. The sedimentary layers of the upper member consist of fanglomerates, sandstones, and siltstones. The phenoclasts are mainly constituted by light colored ignimbritic and rhyolitic fragments similar to the volcanic layers of the APF, and minor greenish and reddish andesitic and metamorphic fragments, compositionally similar to the substratum. East of the Aroma flexure, the sedimentary layers that cover each one of the ignimbritic intercalations show a channel development with meandric pattern, whereas immediately west of the Aroma flexure, the sedimentary layers develop progressive unconformities or are conformably deposited on the underlying ignimbrite (see section 4.2).

[21] On the eastern side of the Precordillera, ~100-m-thick rhyolitic lavas interfinger to the west with the upper member of the APF (Figure 4). The lavas are constituted by crystalline fragments of quartz (50%), sanidine (40%), and minor biotite and plagioclase immersed in a fluidal glassy groundmass. The composition of these lavas and of the ignimbrites suggests that they derive from the same volcanic centers. The rhyolitic lavas overlie the Paleozoic basement and represent the oldest Cenozoic volcanic rocks in the studied area: 26.0 ± 0.4 Ma (Table 1). This age would correspond to the onset of volcanism during late Cenozoic, and it is equivalent to other ages obtained in northern Chile (see Table 1). Nevertheless, the age of the lowermost deposits of the APF is somewhat older, because the lower

member of the APF in the study area onlaps on the Aroma flexure and is overlain by the rhyolites. On the basis of the calculation of sedimentation rate, *García* [2002] proposed that the onset of sedimentation of the Azapa Formation would have begun after 34 Ma in the Arica region. *Victor et al.* [2004] proposed a similar age for the beginning of deposition of the APF in the Altos de Pica region (~27–29 Ma). The uppermost ignimbritic layer of the APF (Nama ignimbrite) was dated by *Muñoz and Sepúlveda* [1992] at 16.2 ± 0.7 Ma in the Camiña valley (Table 1) bracketing the age of the APF (as defined in this paper) between the Oligocene and the early Miocene.

3.2.2. El Diablo Formation

[22] The El Diablo Formation (EDF) is the uppermost sedimentary cover in the Precordillera and displays the characteristic morphology of the western flank of the Altiplano in northern Chile: the Tarapacá Pediplain. This unit is a sequence of fluvial-alluvial conglomerates and sandstones [*Parraguez*, 1998; *Tobar et al.*, 1968]. It is disposed along the Precordillera and Central Depression along a west-to-east distance on more than 45 km. To the east, the EDF interfingers and grades into middle Miocene andesitic lavas (Cerro de Sotoca lavas in the study area). To the west, the distal layers of the EDF onlap over the east slope of the Coastal Cordillera. In the study region, we subdivide the EDF into two members according to its lithological features. This subdivision is similar to the subdivision of the EDF made in the Azapa valley next to Arica [*Parraguez*, 1998].

[23] The lower member is made up of conglomerates, breccias and layers mainly composed by light ignimbritic fragments with minor sandstones beds of similar composition of the underlying units. To the east, this member wedges out on the western limbs of the Aroma flexure (southern study area) or Soga flexure (northern study area) (Figure 5). The upper member is a sequence of semilithified gray conglomerates interbedded with sandstone and marginally by mudstone lenses. Before it wedges out to the east, the upper member interfingers with the andesitic lavas of the Cerros de Sotoca volcanic complex (Cerro Chusmiza according to *Wörner et al.* [2000]). The Cerros de Sotoca lavas correspond to pyroxene andesites, constituted by euhedral plagioclase, pyroxene and minor magnetite included in a glassy groundmass. The compositional similarity of the most of the clasts in the upper member of the EDF and the andesitic lavas derived from the Cerros de Sotoca, and the contact relationship between these lavas and the upper member of the EDF, suggests that this volcanic center is the main source for the clastic components of the upper member of this formation. This relationship was already observed by *Tobar et al.* [1968] and *García* [2002] in the Arica region. The last author grouped the lavas into the Zapahuira Formation.

[24] The main lithofacies of the El Diablo Formation are summarized in Table 2. On the basis of the sedimentary features of the EDF (Table 2), we interpret that debris flows and sporadic gravity flows of sand dominated the proximal zone (between the Cerros de Sotoca volcanic center and the Aroma flexure) of the lower member, whereas turbulent

channelized flows and braided rivers dominated the medial-distal zones (west of the Aroma flexure), according to the models of *Miall* [1985, 1996].

[25] For the upper member, we interpret that the deposits of the proximal zone would have been related to both high- and low-strength debris flows according to the models of *Miall* [1985, 1996]. Ashy matrix and large angular volcanic clasts immediately adjacent to the volcanic edifices suggest that high-strength flow facies could have been triggered by volcanic eruptions, and leading to snow melting in the upper part of the volcanoes [*Sayés*, 1978]. Low-strength debris flows would be the result of hillslope stabilization after eruptions. Laterally limited sand flows with erosive bases would be the result of incipient channel formation. In the medial-distal zone, sedimentary features suggest the formation of elongated or longitudinal conglomeratic bed forms, containing some sandy bed forms and overbank deposits. These features can be interpreted as resulting from braided rivers and turbulent channelized flows according to the models of *Miall* [1985, 1996]. In conjunction, all the features presented for the EDF suggest that this unit represents the development of great coalescent alluvial fans, grading from debris flow-dominated proximal facies, to braided river dominated medial-distal facies, and to fluvial-alluvial plains evaporitic facies in the distal zone, according to the observation of *García* [2002], *Parraguez* [1998], and *Pinto et al.* [2004] in the Central Depression between the Lluta ($18^{\circ}30'S$) and Camiña ($19^{\circ}15'S$) valleys. These features and the great longitudinal extension of the deposits (over 45 km from west to east) can be interpreted as the result of the development of braided fluvial fans, in the sense of *Stanistreet and McCarthy* [1993].

[26] In the Camiña valley (~20 km north of the study region), an 8–9 Ma andesitic lava overlies the EDF (9.0 ± 1.0 Ma [*Naranjo and Paskoff*, 1985] and 8.2 ± 0.7 Ma [*Muñoz and Sepúlveda*, 1992]; see Table 1). Considering the age of the uppermost ignimbrite of the APF (16.2 ± 0.7 Ma), the EDF is comprised between ~16 Ma and 8–9 Ma. This age is similar to the one proposed by *García* [2002] for the EDF in the Arica region. A K/Ar age (whole rock) of 11.7 ± 0.4 Ma was obtained (Table 1) for the lower andesitic lavas interfingering with the lower part of the upper member of the EDF immediately west of the Cerros de Sotoca volcanic complex (Figure 4). This age is similar to the one obtained by *Mortimer et al.* [1974] near Chusmiza (11.3 ± 0.3 Ma, K/Ar, whole rock). In this way, the approximate age of the contact between the lower and upper members of the EDF is 12 Ma.

3.3. Post-8 Ma Deposits and Morphostratigraphic Units

[27] The lavas of the Tatajachura volcano, located north of Jaiña and Chiapa (Figures 4 and 6), overlie directly the substratum and the EDF. These lavas mark the end of the volcanic activity in the eastern Precordillera and western side of the Western Cordillera [*Wörner et al.*, 2000]. The unconformable basal contact of these lavas is a flat surface (Figure 6b). This feature suggests that the volcanic activity occurred after the pediplanation, but before the beginning of

Table 2. Main Lithofacies of the El Diablo Formation

	Lithology/Texture	Sedimentary Features	Observations	Interpretation
<i>Lower Member</i>				
Proximal facies	matrix- and clast-supported subangular gravel	10- to 20-m-thick banks, poorly inverse grading, erosive, and nonerosive base and top	gravel grain size varies between cobble and boulder (proximal facies) and between pebble and cobble (medial-distal facies)	debris flow
Proximal facies	pebbly sand	1-m-thick banks, massive lamination		sporadic gravity sand flows
Medial-distal facies	matrix-supported sandy gravel and clast-supported gravel	5- to 10-m-thick banks, crude stratification and poorly inverse grading		elongated and longitudinal conglomeratic bed forms
Medial-distal facies	fine to coarse sandstone	5- to 20-m-thick banks, planar cross bedding		
Medial-distal facies	mudstone	centimetric lenses, massive, desiccation cracks		
<i>Upper Member</i>				
Proximal facies	matrix-supported gravels and clast-supported gravels	5- to 20-m-thick banks, angular boulder-cobble clast size, massive to crude inverse grading	Large clast (1–3 m of diameter) close to the interfingering lava layers, gray ashy matrix	high- and low-strength debris flows
Medial-distal facies	matrix- and minor clast-supported gravels	15- to 40-m-thick banks, crude horizontal bedding, incipient imbrication	elongated clasts aligned in the imbrication direction (270–200°)	elongated and longitudinal conglomeratic bed forms
Medial-distal facies	Fine sandstone	<10-m-thick banks, low-angle cross bedding and planar cross bedding		sandy bed forms and overbanked deposits
Medial-distal facies	mudstone	centimetric lenses, fine laminated, desiccation cracks		overbanked deposits

incision in the Precordillera. On the basis of morphological similarities with other volcanic edifices (smooth cone shapes), *Wörner et al.* [2000] suggested a lower Pliocene age for the volcanic edifice. However, we believe that its age could be somewhat older, considering the age of pediplain (younger than 8–9 Ma) and the beginning of incision in the Precordillera (circa 7 Ma, see below).

[28] East of the Aroma flexure, discontinued gravel deposits are preserved on the hillslope of the Aroma valley, between 300 and 600 m above the bottom of the valley (Figure 6b). These deposits (San Antonio Conglomerates of *Fariás* [2003]) form a 300-m-thick series of planar-stratified subhorizontal matrix-supported conglomerates interbedded with centimetric sand layers. The conglomerates correspond to terraces deposits possibly associated to thalweg slope stabilization during the valley formation. In contrast, west of the Calacala flexure, strath (erosional) terraces (in the sense of *Burbank and Anderson* [2001]) are excavated on the pediplain (Figure 6d).

[29] In the Central Depression, after crossing the boundary with the Precordillera, the Aroma valley changes its orientation from $\sim 250^\circ$ to $\sim 200^\circ$. East of the southward trending segment of the Aroma valley (Figure 6e), several abandoned valleys cross the strath terraces. These abandoned valleys gradually change their orientation from north to south from 280° to 250° (Figure 6e). To the west, beyond the boundary between the Precordillera and the Central Depression, nearly all of these valleys can be associated

with alluvial fan deposits that often reach the eastern flank of the Coastal Cordillera (Figure 6a). The deposits of the present-day Aroma alluvial fan as well as those of the Tarapacá valley are SSW oriented (Figure 6a).

[30] Both aggradational and erosional terraces, as well as alluvial fans developed west of the channelized zone of the valleys flowing down from the Precordillera, show progradation of deposition during incision. Furthermore, the anticlockwise rotation of the valley orientation next to the boundary between the Precordillera and the Central Depression evidences a southward tilting of the Central Depression in this region after or coeval to the beginning of the incision on the western flank of the Altiplano.

4. Tectonic Deformation

4.1. Structural Mapping

[31] In the study region, the major tectonic features affecting the Cenozoic cover consist of three west dipping monocline folds or flexures (Figures 4 and 5). Syntectonic deposition of gravels and ignimbrites resulted in the development of growth strata along the flexures (Figures 7 and 8). From west to east, the main flexures are known as: Calacala, Aroma, and Soga. Two smaller flexures are exposed west of the main ones (Figure 4).

[32] A general change in the trend of the flexure system occurs at the Aroma valley (Figure 4). The trends of the

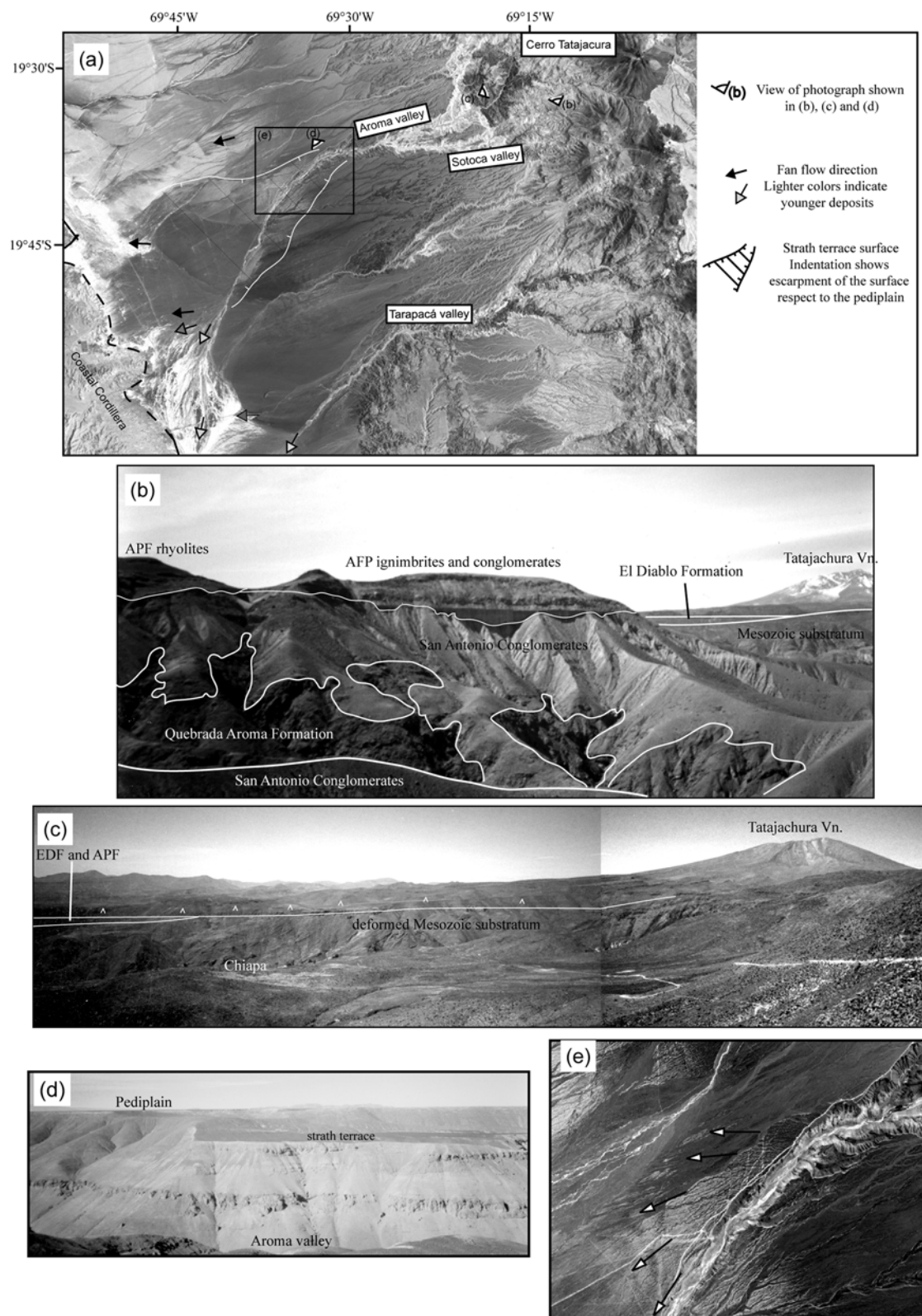


Figure 6

Calacala and Soga flexures change gradually from N25°W to N20°W and from N35°W to N10°W, respectively. The trend change of the Aroma flexure occurs at the headwater of the Yalañuzco valley; there its orientation steeply changes from N35°W to N-S. The width of the steep western limbs of these flexures is larger in the Calacala flexure (~4 km), whereas it is about 1 km and 800 m in the Aroma and Soga flexures, respectively. This bending of the Precordilleran structure, from N-S, to the south, to NNW-SSE, to the north, correlates with the major bending of the central Andes (Figure 1b), because it is located near the symmetry line of the Bolivian Orocline [Gephart, 1994].

[33] North of the Soga valley, the prolongation of the Aroma and Soga flexures is westwardly displaced by the oblique Soga fault (Figures 9 and 10). The strike and dip of this fault is N80°W/30–40°N in its southeastern segment and N45°W/50–60°NE in its northwestern segment (Figure 4). Apart from the westward displacement of the flexures, kinematic indicators (drag folds and striae) and the fact that the northeastern block of this fault is up thrust (Figure 9) indicate a sinistral reverse motion. The maximum observed throw is about 350 m. The northern prolongation of the Aroma flexure, which is named the Moquella flexure [Muñoz and Sepúlveda, 1992; Pinto *et al.*, 2004], is displaced ~5 km to the west by this fault. The northern prolongation of the Soga flexure, in the deeply incised Camiña valley, is a less developed reverse fault (Quisama fault of Pinto *et al.* [2004]), which is also displaced about 5 km to the west by the Soga fault. The western Calacala flexure is not affected by the Soga fault. The northern prolongation of the Calacala flexure is the Tana flexure [Pinto *et al.*, 2004], north of the Camiña valley (Figure 10). The prolongation can be traced easily on the interfluvial pediplain as to the parallel drainage east of the flexure tends to converge next to the axis of the flexure, and because alluvial sediments deposited immediately toward the west of the flexure (Figure 10). The southern prolongation of the flexures can be traced up to the Tarapacá valley. Along this valley, complex deformation involves the substratum and the Cenozoic cover (Figure 10). Different pattern of flexures north and south of this valley suggest that the Tarapacá valley follows an E-W transfer zone.

[34] Secondary structures are developed in association with the flexures; these structures have the same trend as the monoclines. On the crest, they correspond to extensional fractures filled with silica veins. On the western limbs, minor reverse faults, both west and east vergent, occur with the same strike of the flexures; offsets caused by these faults are smaller than 10 m. According to the models of Ameen [1988], such features suggest that the flexures are the result of the propagation of blind west vergent reverse faults, and

that the minor reverse and normal faults correspond to intrafold accommodation structures. Furthermore, overturned basal layers of the APF on the Aroma flexure (~85°E dipping) indicate shortening perpendicular to the fold strike.

[35] In the Yalañuzco valley, which runs along the hinge line of the Aroma flexure, folded Paleozoic metasedimentary rocks of the Quebrada Aroma Formation present mylonitic deformation, parallel to the trend of the Aroma flexure. The main planar foliation is vertical and oriented N-S to N40°W (Figure 11). Unrooted and intrafolial folds have vertical and horizontal axes. The observed width of the mylonite zone in the valley is ~40 m. The Paleozoic rocks are intruded by Mesozoic dikes that have the same orientation as the mylonite. These dikes are cut by ~N20°W/50°E oriented faults developing striae that indicate reverse dextral motion along these faults. Furthermore, prograding alluvial fans developed during the valley incision are intensely fractured by subvertical N-S to NW-SE oriented cracks, indicating instability along the sides of the valley, and possibly recent tectonic activity (Figure 11). According to our field observations, most of the cracks (even the mud that after the last rains recovered some outcrop surfaces is cracked), landslides and rockfalls in the Yalañuzco valley were caused by the Aroma earthquake and its aftershocks.

4.2. Geometric Analysis of the Growth Strata

[36] The analysis of growth strata developed on syntectonic deposits allow to understand the behavior of the structural evolution of growth folds, such as the relative rates of uplift and deposition, and constrain the different period of activity. [Burbank and Vergés, 1994; Ford *et al.*, 1997; Riba, 1976].

[37] In the study region, the deposits mainly display overlap geometries on the western flank of the flexures, often overlain by off-lapping and on-lapping layers (Figure 8). Following the models of Burbank and Vergés [1994], overlap geometries occur when the accumulation rate is greater than the relative surface uplift rate, off lap occur when the relative uplift rate was greater than the accumulation rate. Onlap appears following off-lap geometry, suggesting a change to more rapid accumulation rates in comparison with uplift rates. Detailed mapping of these geometries shows that minor surface aggradation (off-lap and onlap geometries) is mainly related to sedimentary deposition, whereas major surface aggradation (overlap geometry) is associated with ignimbritic deposition (Figure 8).

[38] Restoration of the predepositional geometry of the Cenozoic series was made considering the altitude difference of each key bed between the crest and foot of each flexure. The key beds selected for restoration correspond to

Figure 6. Post-8 Ma deposits and morphostratigraphic units. (a) Landsat 7 mosaic image (available at <https://zulu.ssc.nasa.gov/mrsid/>). (b) View of the San Antonio conglomerate preserved on the hillslope of the Aroma valley. (c) View of the unconformity between the Mesozoic substratum, the Altos de Pica and the El Diablo formations, and the Tatajachura lavas. (d) Strath terraces developed on the Tarapacá Pediplain over the Aroma valley. (e) Aster image that shows anticlockwise rotation of the Aroma valley on the limit between the Central Depression and the Precordillera displayed by abandoned channels directions.

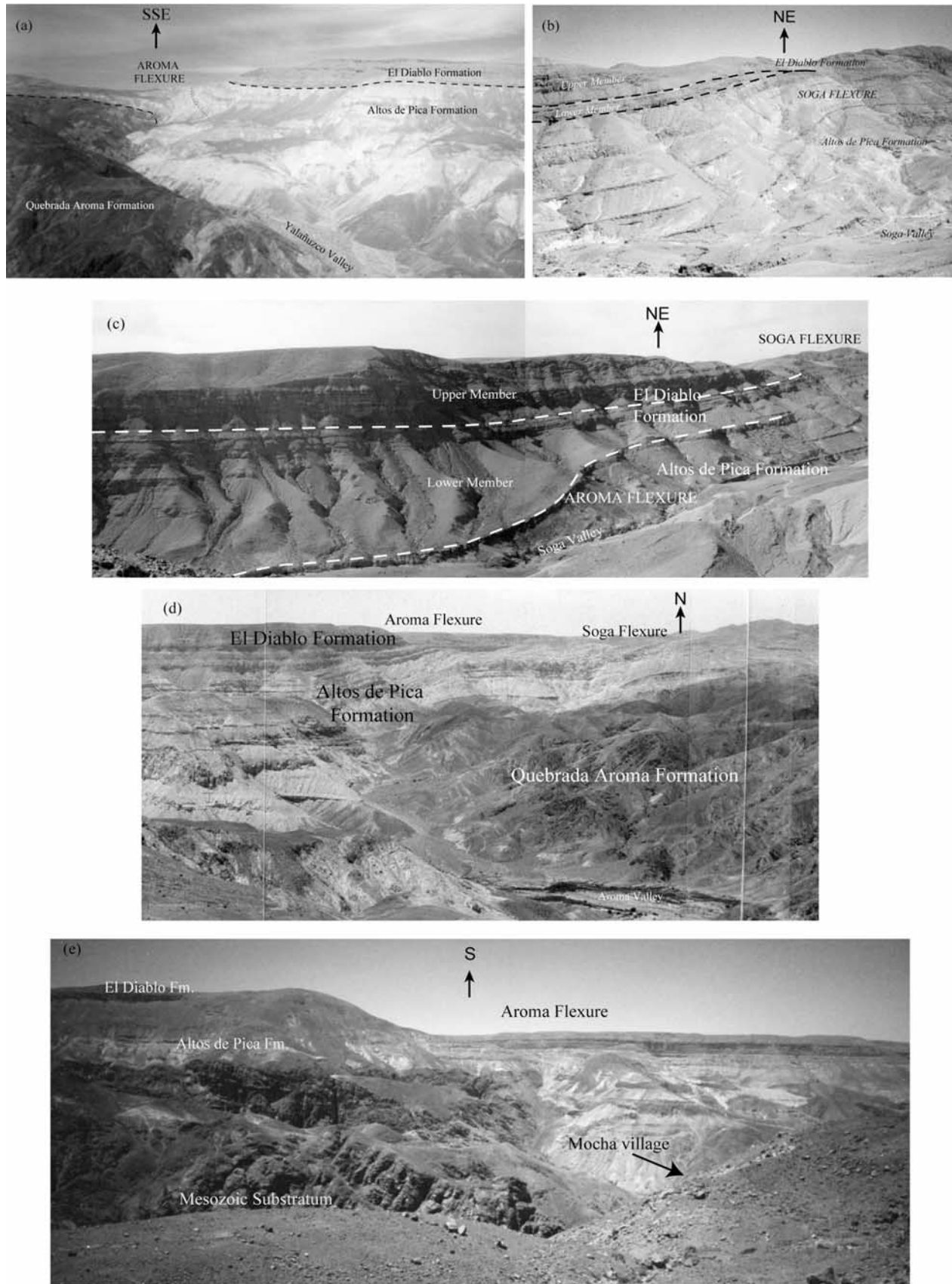


Figure 7

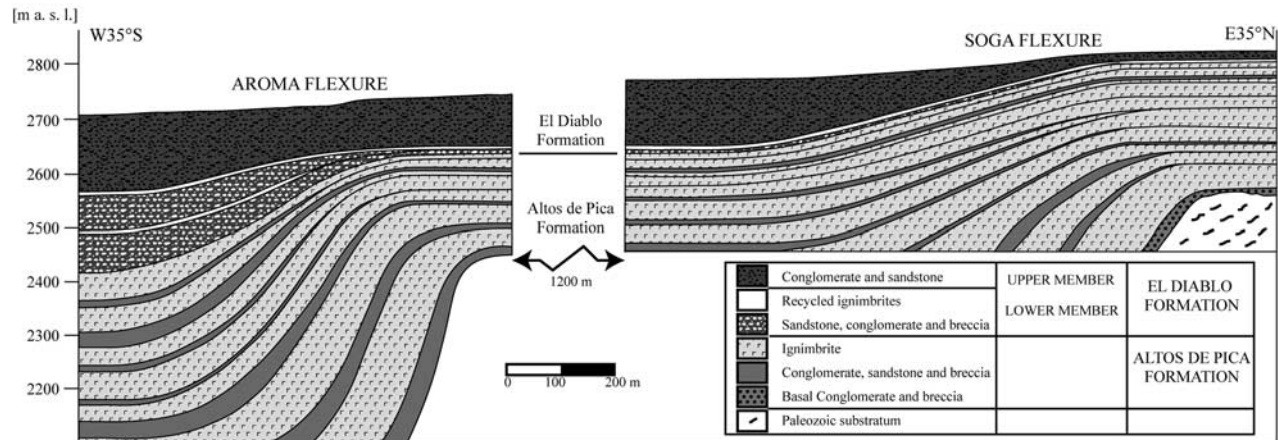


Figure 8. Detailed cross section in the Soga valley. The growth strata developed on the Aroma and Soga flexures are shown.

(1) the contact between the substratum and the APF; (2) the contact between the APF and the base of the EDF, (3) the contact between the lower and upper members of the EDF; and (4) the top of the EDF. Measuring the altitude difference between each one of these key beds on both sides of the flexures allowed us to constrain the evolution of the flexures into four stages of deformation: (1) 26–16 Ma (APF deposition); (2) 16–12 Ma (lower EDF deposition); (3) 12–8 Ma (upper EDF deposition); and (4) 8–0 Ma (post-EDF deposition). Although we use the 26 Ma age for the beginning of the first stage (the oldest age obtained for the APF in the study region), this age could be somewhat older, because the onset of contractional deformation in the central Andes Altiplano [Sempere *et al.*, 1990] and the age of accumulation of the APF [García, 2002; Victor *et al.*, 2004] has been estimated as circa 30 Ma (see also section 3.2.1).

[39] The relative surface uplift registered on the Aroma and Soga flexures since 26 Ma is about 700 and 420 m, respectively (Figures 8 and 12). On the Calacala flexure and the minor western flexures the relative surface uplift calculated is about 640 and 150 m, respectively, although it could be larger because the lower layers of the Cenozoic sequence do not crop out in this part of the study region. During the first stage (26–16 Ma), the relative surface uplift accommodated by the three main flexures is 1010 m, at a rate of 0.10 mm/yr. During the second and third stages, the relative surface uplift is 360 and 350 m, respectively, both at a rate of 0.09 mm/yr. Since 8 Ma (fourth stage) the relative uplift is 190 m, at a slower rate of 0.02 mm/yr. The relative surface uplift

calculated for each flexure during each stage is summarized in Table 3. Since 26 Ma, the total relative uplift accommodated by the flexure system is larger than 1900 m. Relative uplift during the first stage mainly concentrated on the eastern structures, whereas in the last stages, it concentrates on the western structures, showing a westward migration of the main front of deformation (Figure 13). Furthermore, the relative uplift rate decreases from ~ 0.1 to 0.02 mm/yr during the last stage. This period (8–0 Ma) corresponds to the end of deposition in the Precordillera, and coincides with an important aridification episode, the stage of pediplain formation [Mortimer, 1980], and the shift of the volcanic arc to its present-day location [e.g., Wörner *et al.*, 2000], with the exception of the Mamuta ($\sim 19^{\circ}15'S$) and Tatajachura volcanoes (see Figure 2 for location).

4.3. Seismological Analysis

[40] In northern Chile, between Arica and the Mejillones Peninsula ($\sim 18^{\circ}30'S$ – $23^{\circ}S$), major interplate earthquakes ($M > 8$) occurred in 1545, 1615, 1768, and 1877, with an average recurrence period of 111 ± 33 years [Comte and Pardo, 1991]. Major interplate earthquakes in southern Peru have been more frequent than in northern Chile; they occurred in 1513, 1604, 1687, 1715, 1784, and 1868 and recently on 23 June 2001 ($M_w = 8.4$). The rupture area of the southern Peru 2001 earthquake ended in Ilo ($17^{\circ}40'S$). The region between Ilo and the Mejillones Peninsula remained intact for more than a century. Therefore, in this region, a large earthquake along the interplate contact is expected to occur soon [Comte *et al.*, 2002].

Figure 7. Photographs of the Aroma and Soga flexures. (a) View of the Aroma flexure in the Yalañuzco valley. (b) View of the Soga flexure in the Soga valley. (c) View of Aroma (left) and Soga (right) flexures in the Soga valley. (d). View of both flexures from the headwater of the Yalañuzco valley. (e). View of the Aroma flexure in the Tarapacá valley next to Mocha. Note that the dip of the substratum follows the same style as the deformation of the Cenozoic series. See color version of this figure at back of this issue.

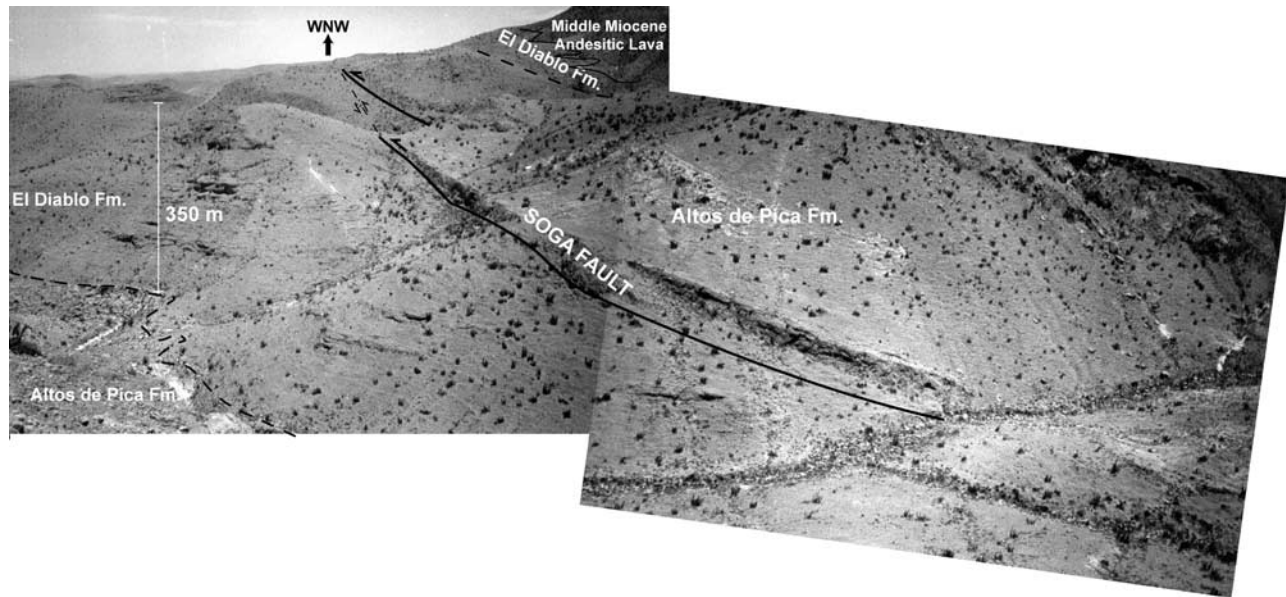


Figure 9. View of the Soga fault in the northern part of the study area.

[41] Several small magnitude shallow crustal seismic events in the continental forearc have been detected in the last decade. On the basis of microseismicity data recorded by the permanent network of Arica (18°S – 19°S), *David et al.* [2002] reveal the existence of a west dipping structure in the continental forearc. This structure extends from the Wadati-Benioff zone below the Central Depression (~ 60 km deep) to the top of the crust in the eastern side of the Western Cordillera. The stress tensor determined by *David et al.* [2002] using 30 well-constrained focal mechanisms, with depths between 30 and 60 km, suggests that the west dipping alignment of earthquake hypocenters corresponds to an east vergent reverse fault.

[42] One month after the southern Peru earthquake (23 June 2001), a shallow crustal earthquake occurred below the Precordillera of northern Chile (24 July 2001, $M_w = 6.3$, Aroma earthquake) with a major aftershock on 14 January 2002 (Chusmiza earthquake, $M_w = 5.9$) (Figures 1 and 14). Crustal seismicity in the Aroma region was almost absent before the southern Peru interplate earthquake, and just a few events occurred before 24 July 2004 [*Comte et al.*, 2003a]. This suggests a strong temporal and spatial relationship between the crustal deformation in the Precordillera and the interplate seismic activity in the Arica Bend region [*Martinod et al.*, 2002].

[43] The Aroma earthquake is the first major shallow crustal earthquake recorded by seismological and accelerographic networks in Chile. Its hypocenter is ~ 10 km deep, next to the Aroma locality (Figures 4 and 14). Its epicenter is therefore located at the bend of the Aroma flexure. The Harvard centroid moment tensor (CMT) focal mechanism corresponds to a strike-slip solution, either to a dextral $\sim \text{N-S}$ or a sinistral E-W displacement, the p axis being nearly coincident with the plate convergence direction of NUVEL-1A [*DeMets et al.*, 1994]. Table 4 summarizes the

most important data for the southern Peru, Aroma, and Chusmiza earthquakes released by the Harvard CMT.

[44] Aftershocks were recorded by the permanent seismological and telemetrical network of northern Chile (RESISTE-ARICA) and by two temporal seismological stations with three components (see Figure 2 for location). In this study, we use the July–October 2001 data recorded by these stations. The aftershock sequence can be subdivided into two segments, according to their location north or south of the Aroma earthquake epicenter (Figure 14). Aftershocks corresponding to the southern segment are distributed in a N-S oriented line, which is relatively coincident with the orientation and location of the southern segment of the Aroma flexure. North of the Aroma earthquake epicenter, the number of aftershocks is greater than south of it and their distribution is rather scattered (Figure 14). Aftershocks south of the epicenter show a high-angle east dipping structure until 25 km depth, along a 20 km trace, which implies a rupture area of ~ 500 km².

[45] On the basis of the aftershock locations, we suggest that the 24 July 2001 earthquake may have reactivated an ancient basement fault, locally visible in the Paleozoic substratum in the Aroma valley. This same fault seems to have controlled the position and geometry of the late Oligocene–Neogene Aroma flexure. The dispersion of aftershocks in the northern segment could be the result of the adjustments of crustal blocks separated by the bending of the flexure. The existence of the WNW–ESE trending Soga fault, immediately north of this rupture area, suggests that some strike-slip deformation could be transferred to this structure, which is almost perpendicular to trend of the flexures, causing the thrusting of the northern block over the southern block. In addition, WNW–ESE sinistral displacement observed in the Soga fault could be the conjugate

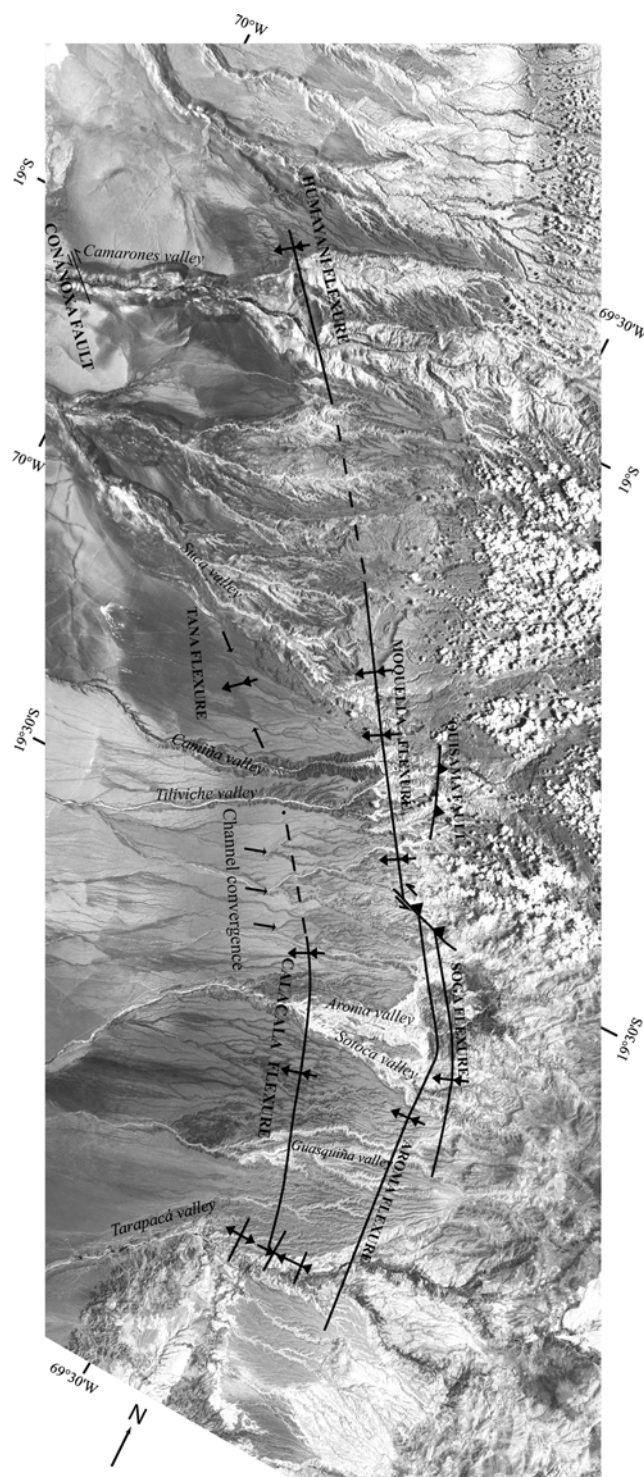


Figure 10. Landsat 7 mosaic image of the Precordillera of northern Chile (available at <https://zulu.ssc.nasa.gov/mrsid/>) that shows the continuity of structures along the western side of the Altiplano. Huayamani flexure and Cananoxa fault are reported by *García* [2002], and Moquella and Tana flexures and Quisama fault are reported by *Pinto et al.* [2004]. Flexures can be followed to the Tarapacá valley, where complex deformation affects the Mesozoic substratum and the Cenozoic cover.

solution of the N-S dextral strike slip inferred for the Aroma earthquake.

5. Discussion

5.1. Structural Configuration of the Western Flank of the Altiplano: A Crustal-Scale Fault Bend Fold

[46] The spatial relationship between the system of flexures described here and the shallow seismicity suggests that the Aroma earthquake and its aftershocks occurred along the essentially blind fault that controls the development of the Aroma flexure. The trace of this fault locally appears in the Yalañuzco valley. Field data indicate that this fault constitutes a long-lasting weakness zone. The rocks affected by the fault exhibit both ductile and brittle deformation. Ductile deformation (mylonitization) affected the Paleozoic Quebrada Aroma Formation and brittle deformation affects the overlying Cenozoic deposits. According to *Harambour* [1990, and reference therein], in Sinemurian to lower Oxfordian times, this fault, as well as the structural system in the Aroma region, accommodated extensional tectonics, whereas during Oligocene-Miocene times it accommodated contractional strain, and strike slip according to the here presented interpretation of the recent shallow seismic activity. During the late Oligocene-Neogene and before 8 Ma, we propose that this fault has been reactivated essentially as a west vergent thrust fault. After 8 Ma, geological and morphological data described above show that the vertical relative surface motion accommodated by the flexure system slowed down. This slowing has been also observed in the Altos de Pica area by *Victor et al.* [2004] as well as in the Arica region [*García*, 2002]. The dynamics of that part of the Andean forearc changed at that time with the onset of the westward forearc tilting that would have triggered the incision that formed the deep valleys within the Precordillera in northern Chile (see section 5.2). The transcurrent reactivation of the fault by the Aroma 24 July 2001 earthquake shows that the present-day tectonic regime differs from that prevailing during the lower and middle Miocene.

[47] Seismological data show that the Aroma earthquake strike slip occurred on a steep east dipping fault that continues downward to ~25 km depth (Figure 15). The high-angle east dipping geometry of the faults in the Precordillera of northern Chile seems to be a constant feature, confirming the observation made by *Muñoz and Sepúlveda* [1992] and *Muñoz and Charrier* [1996]: in the Precordillera of Arica, *García* [2002] concluded that the Ausipar fault is very steep (~60°E dipping); in the Altos de Pica region, based on quantitative reconstruction of the thrust system in the Precordillera, *Victor et al.* [2004] suggested that the deep continuation of this system is better represented by a ramp dipping steeper than 45° to the east.

[48] At the latitude of the Altos de Pica region (~21°S) seismic reflection profiles and geophysical experiments show the presence of a <30-km-deep west dipping reflector below the Precordillera (Quebrada Blanca Bright Spot) associated with a low-velocity zone, *P* to *S* wave conversions, and corresponding to the upper boundary of a high

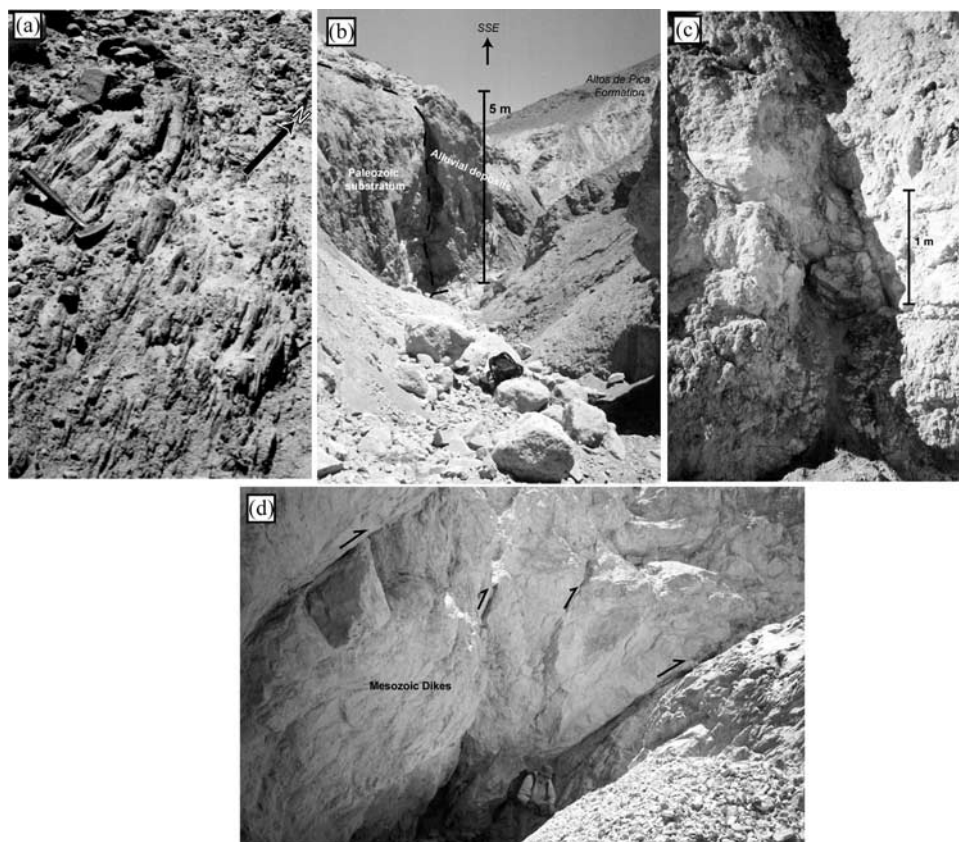


Figure 11. Photographs in the Yalañuzco valley. (a) Foliation in Quebrada Aroma Formation. In the center of the fold, the material is uprooted. The main foliation is similar to the Aroma flexure trend in this locality (NNW-SSE). (b) Tributary aligned with major fractures cutting the substratum and recent deposits. (c) Close up of a fracture that cuts the recent alluvial deposits. (d) Mesozoic dikes intruding the Quebrada Aroma Formation. These dikes are delimited and cut by east dipping faults that present reverse dextral kinematic indicators.

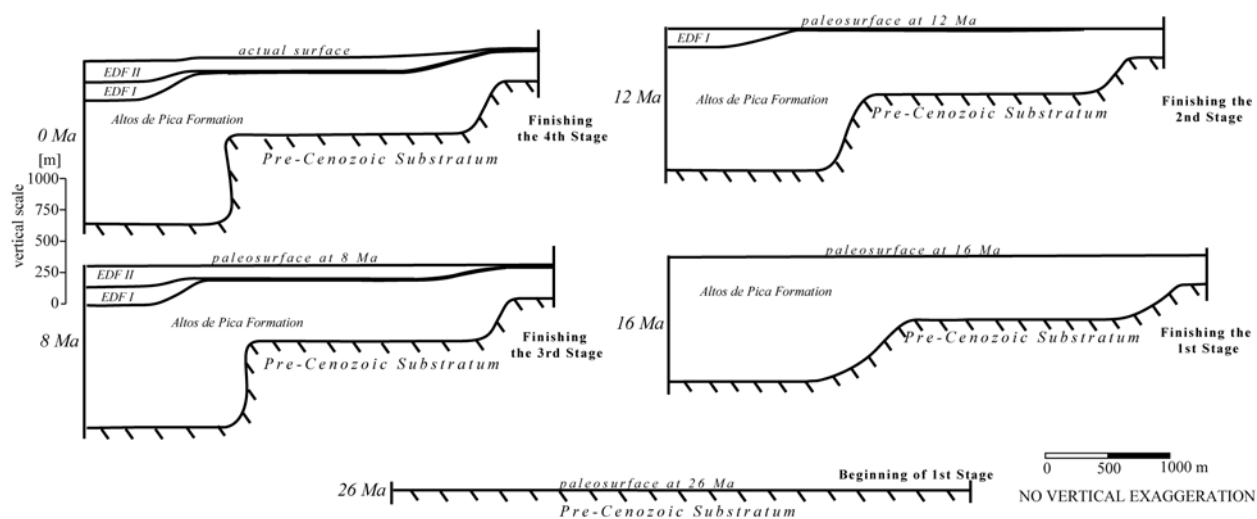


Figure 12. Structural restoration of the Aroma and Soga flexures since 26 Ma until present-day.

Table 3. Relative Uplift Data for the Flexures During the Four Stages of Deformation in the Study Area^a

Flexure	Soga	Aroma	Calacala	Minor	Total
<i>First Stage, 26–16 Ma</i>					
Relative uplift, m	260	500	250	?	1010
Rate, mm/yr	0.03	0.05	0.03	?	0.10
<i>Second Stage, 16–12 Ma</i>					
Relative uplift, m	10	150	200	?	360
Rate, mm/yr	<0.01	0.04	0.05	?	0.09
<i>Third Stage, 12–8 Ma</i>					
Relative uplift, m	120	30	100	100	350
Rate, mm/yr	0.03	0.01	0.03	0.03	0.09
<i>Fourth Stage, 8–0 Ma</i>					
Relative uplift, m	30	20	90	50	190
Rate, mm/yr	<0.01	<0.01	0.01	0.01	0.02

conductivity and high Poisson's ratios domain [ANCORP Working Group, 2003]. ANCORP Working Group [2003] favored the idea that the Quebrada Blanca Bright Spot is a petrophysical feature related to the presence of fluids or melts, or mafic intrusions into a felsic country rock. Victor *et al.* [2004] suggest that the western termination of this reflector corresponds to the downdip end of the west vergent thrusts outcropping in the Altos de Pica area. The discontinuity continues farther to the east, below the Altiplano and Eastern Cordillera between 15 and 30 km depth, where is called the Altiplano low-velocity zone (ALVZ, see Figure 15) [Yuan *et al.*, 2000]. The ALVZ would be related to the brittle-plastic midcrustal transition decoupling mechanically an upper rigid crust from a lower

ductile crust [Yuan *et al.*, 2000; ANCORP Working Group, 2003; Tassara, 2005; Victor *et al.*, 2004].

[49] Therefore both the Quebrada Blanca Bright Spot and the ALVZ reflect rheological change at depth separating two different domains within the crust that may have experienced different strain histories. In particular, lateral ductile flow may have occurred below that boundary to distribute at depth the crustal thickening concentrated near the surface in restricted areas [e.g., Husson and Sempere, 2003]. Although the geophysical analysis does not give information on possible displacements, the mechanic decoupling proposed by several authors for the discontinuity could also make possible relative displacements between the lower and upper crust, facilitating the deep flow of the lower crust (see section 5.5).

[50] Apart from the WTS, the ALVZ and the Quebrada Blanca Bright Spot, other structures have been observed within the forearc and Western Cordillera of northern Chile. On the basis of the distribution of crustal microseismicity in the Arica region, David *et al.* [2002] and Comte *et al.* [2003a] proposed the existence of a west dipping N-S to NNW-SSE oriented fault issued from the Wadati-Benioff zone beneath the Central Depression at a depth of ~60 km and emerging to the surface in the eastern side of the Western Cordillera. David *et al.* [2002] proposed that this structure may correspond to the thermal and rheological boundary between the rigid forearc block and the weak ductile crust of the magmatic arc and of the Altiplano. In this way, this structure seems to be the northern equivalent of the Quebrada Blanca Bright Spot. Inversion of focal mechanisms calculated on 30- to 60-km-deep events shows that below the Central Depression and western Precordillera this structure accommodates horizontal ENE-WSW short-

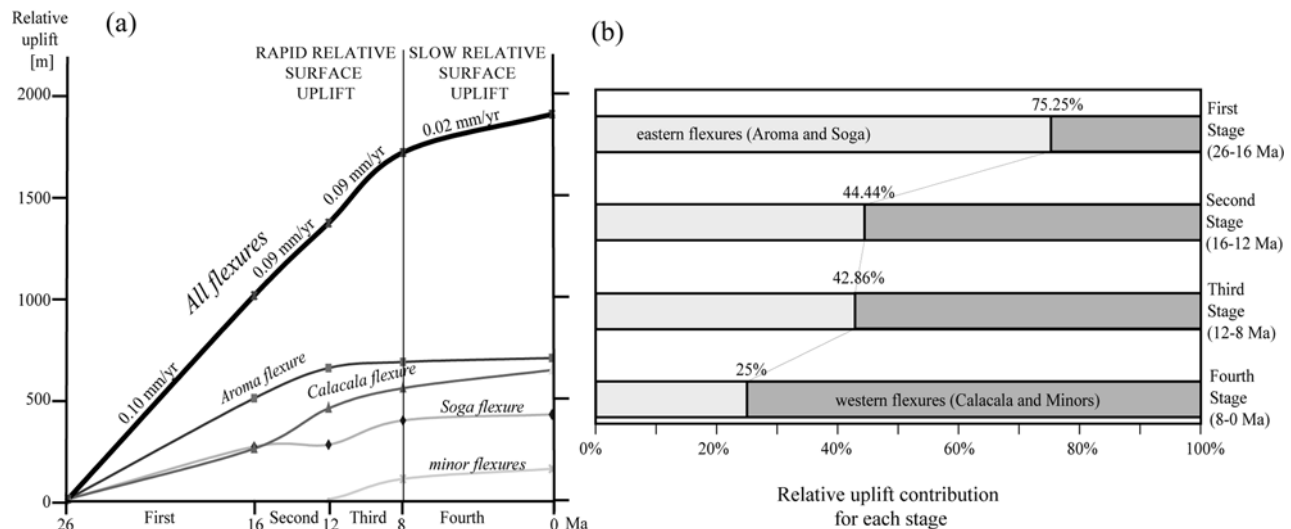


Figure 13. Comparison between the relative uplift contribution of each flexure in the study region. (a) Relative uplift accumulated for each flexure during the four deformation stages. (b) Comparative percentage of relative uplift contribution. It can be observed that during early stages the deformation is concentrated in the eastern flexures, whereas in the slower last stage the deformation concentrates on the western structures.

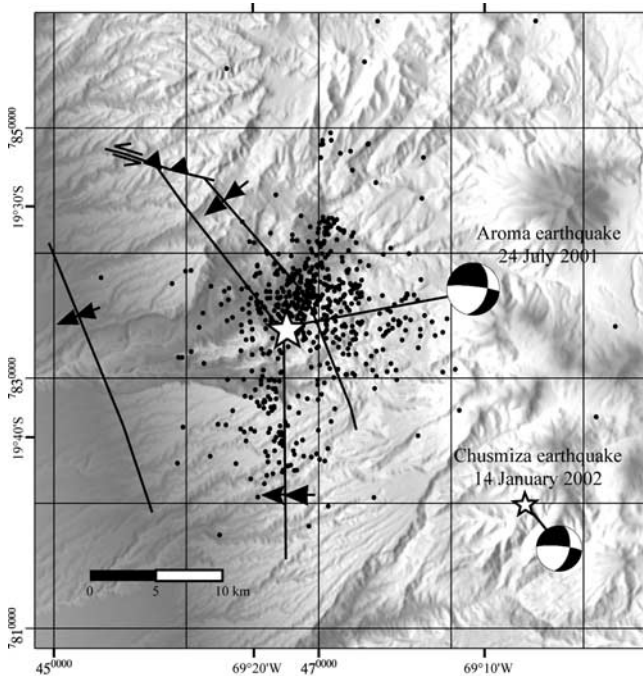


Figure 14. Shallow seismic activity registered from 24 July 2001 to 1 November 2001. Focal mechanisms for the Aroma and Chusmiza earthquake were determined by Harvard CMT (<http://www.seismology.harvard.edu/projects/CMT/>).

ening at depth. Although in the Aroma region we do not find evidence of this west dipping structure, its occurrence north of this area and the presence of the Quebrada Bright Spot about 100 km farther south suggest that this structure could exist below the western flank of the Altiplano at $19^{\circ}30'S$.

[51] In the upward continuation of that structure, in the Western Cordillera of the Arica region, east vergent thrusts outcrop in the Chucal region [Charrier *et al.*, 2002; Riquelme, 1998; Riquelme and Hérail, 1997]. These structures extend southward to $\sim 20^{\circ}S$, where they disappear below the late Neogene-Recent volcanic edifices and deposits (see Figure 2). We consider that microseismic data [Comte *et al.*, 2003a; David *et al.*, 2002] provide strong

evidence that the west dipping discontinuity is a tectonic structure, whose superficial expression corresponds to the east vergent thrusts located in the eastern side of the Western Cordillera.

[52] The activity of the east vergent thrusts was mainly registered on the Neogene sequences in the Western Cordillera before 10 Ma [Charrier *et al.*, 2002], coinciding with the main deformation stage affecting the WTS. Therefore we propose that the Neogene relative surface uplift of the western flank of the Altiplano in northern Chile before 8 Ma was accommodated by a crustal-scale fault bend fold, formed by a major west dipping ramp extending from the Wadati-Benioff zone to the eastern side of the Western Cordillera. The west vergent thrusts described above would correspond to back thrust structures (Figure 15).

[53] After 8 Ma, the vertical displacement accommodated by the WTS slowed down. The relative uplift of the Western Cordillera and Altiplano with respect to the Central Depression resulted in the westward tilting of the Chilean forearc (see below). The 24 July 2001 Aroma earthquake suggests that the system of faults emerging within the Precordillera and Western Cordillera now accommodates dextral strike-slip displacements, as observed at the Altos de Pica latitude by Victor *et al.* [2004] (see section 5.4).

5.2. Late Miocene Tilting and the Beginning of Incision

[54] The deposition of the Tana lava over the EDF in the Camiña region marks the end of the extended sedimentation on the Precordillera of northern Chile at 8–9 Ma [Muñoz and Sepúlveda, 1992; Naranjo and Paskoff, 1985; Pinto *et al.*, 2004]. This event was coeval with a shift of volcanism toward the east from the eastern Precordillera to its present-day location in the Western Cordillera [Wörner *et al.*, 2000]. Furthermore, an important decrease in the activity of the WTS in the Aroma region is registered at this time.

[55] The incision that formed the deep valleys in the Precordillera and Central Depression in northern Chile commenced after 8–9 Ma (age of the lava deposited over the unincisioned pediplain in the Camiña region [Pinto *et al.*, 2004]). Many authors argued that the onset of the incision could have been the result of headward erosion resulting from the transition from an endorheic to an exorheic drainage system [e.g., Mortimer and Saric,

Table 4. Information for the Southern Peru, Aroma, and Chusmiza Earthquakes Generated by the Harvard CMT^a

	Southern Peru Earthquake	Aroma Earthquake	Chusmiza Earthquake
Event	062301E	072401C	011402C
Date	23 June 2001	24 July 2001	14 January 2002
M_w	8.4	6.3	5.6
Scalar moment	4.67×10^{28}	3.58×10^{25}	3.06×10^{24}
Fault plane ^b			
Strike	310/159	14/276	13/275
Dip	18/74	46/82	53/80
Slip	63/98	−169/−44	−167/−37

^aSee <http://www.seismology.harvard.edu/CMTsearch.html>.

^bThe first value is for fault plane solution and the second is for conjugated fault plane solution.

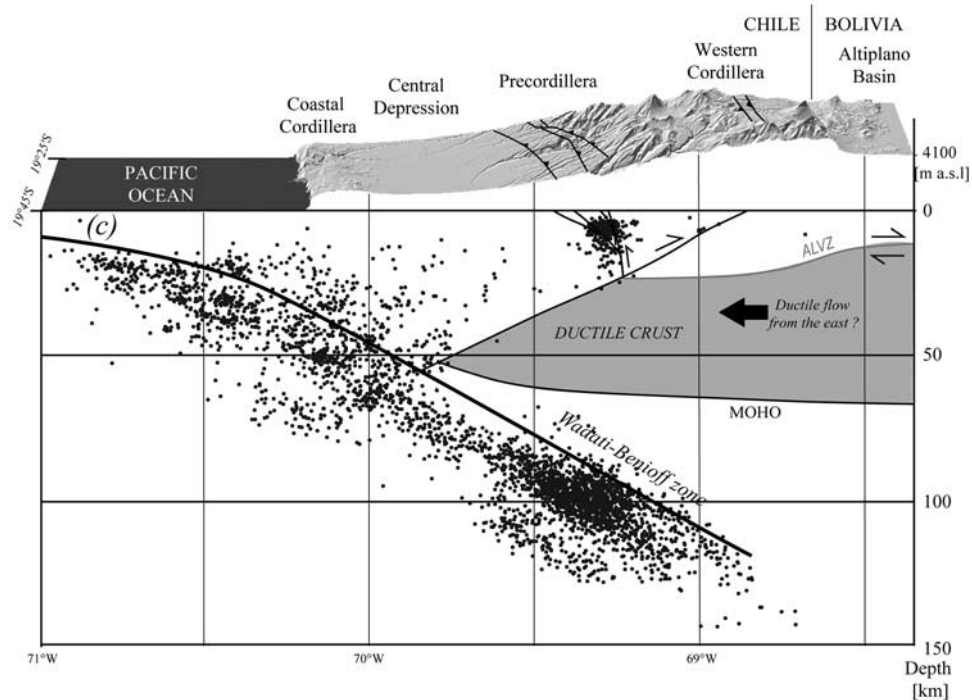


Figure 15. Correlation between the geological structures and the seismicity recorded between 19°25'S and 19°45'S in the western flank of the Altiplano. The geometry in depth of the studied flexure system is based on geometry of the thrusts in the Altos de Pica region [Victor *et al.*, 2004] and in the Arica region [García, 2002]. ALVZ and Moho are based on the works by Dorbath and Masson [2000], Masson *et al.* [2000], Yuan *et al.* [2000], and ANCORP Working Group [2003]. West dipping structure is based on the seismicity recorded in the Arica region [David *et al.*, 2002] and the Quebrada Blanca Bright Spot observed in the Altos de Pica region [ANCORP Working Group, 1999, 2003; Victor *et al.*, 2004].

1972; Naranjo and Paskoff, 1985; Uhlig *et al.*, 1996]. However, the region between the Tiliviche valley and Loa river presents a comparable incision degree in the Precordillera, although it still remains endorheic (Figure 16). North of the endorheic zone, the Coastal Cordillera elevation decreases. In the Camiña and Tiviliche valleys, knickpoint migrations can be observed in the Central Depression. They show that the incision of these valleys in the Precordillera is controlled by the elevation of the Central Depression and that it is not a consequence of a base level fall related to the shift from endorheic to exorheic drainage (Figure 16).

[56] We conclude that the headward incision from the sea is a process that may have contributed to the deepening of valleys north of 19°30'S, but that it does not explain the beginning of incision in valleys south of the Camarones river. Therefore other process must have triggered the incision there. We argue that the incision was triggered by the westward tilting of the Precordillera: the shift from extended fluvial-alluvial fans deposition to dissection in the Precordillera results from the increasing slope of the western flank of the Precordillera. The westward progradation of alluvial fans, as well as degradational terraces developed in the western Precordillera and Central Depression are evidences of relative base

level lowering, that can only result from the relative surface uplift of the Western Cordillera because the drainage system remains closed to the sea. The facies of the EDF suggests giant (more than 40 km long) braided fluvial fan deposition. According to the models of Stanistreet and McCarthy [1993], this kind of fans normally deposit on gentle slopes ($<1^\circ$). The present-day slope of the Precordillera, in contrast, varies between 2 and 4°. Moreover, Gregory-Wodzicki *et al.* [1998] show that the Altiplano and Western Cordillera elevation increased significantly during the late Miocene. Since that period is not marked by important thrust fault activity in the Precordillera, it is probable that the relative uplift of the Cordillera was accommodated by the westward tilting of the western flank of the chain, as already suggested by Lamb *et al.* [1997] (see section 5.4).

[57] Kiefer *et al.* [1997] constrained the age of pediplain dissection in the Precordillera at 21°40'S (catchment of the Arcas fan) between 7.3 ± 0.2 Ma and 6.8 ± 0.2 Ma. On the basis of the age of a cineritic level located in the limit between the Coastal Cordillera and Central Depression (19°32.5'S/69°57.4'W, see Figure 16), Naranjo and Paskoff [1985] suggested that the incision on Tiliviche valley would have begun after 5.5 Ma. This level is located west of the knickpoint that migrates from the

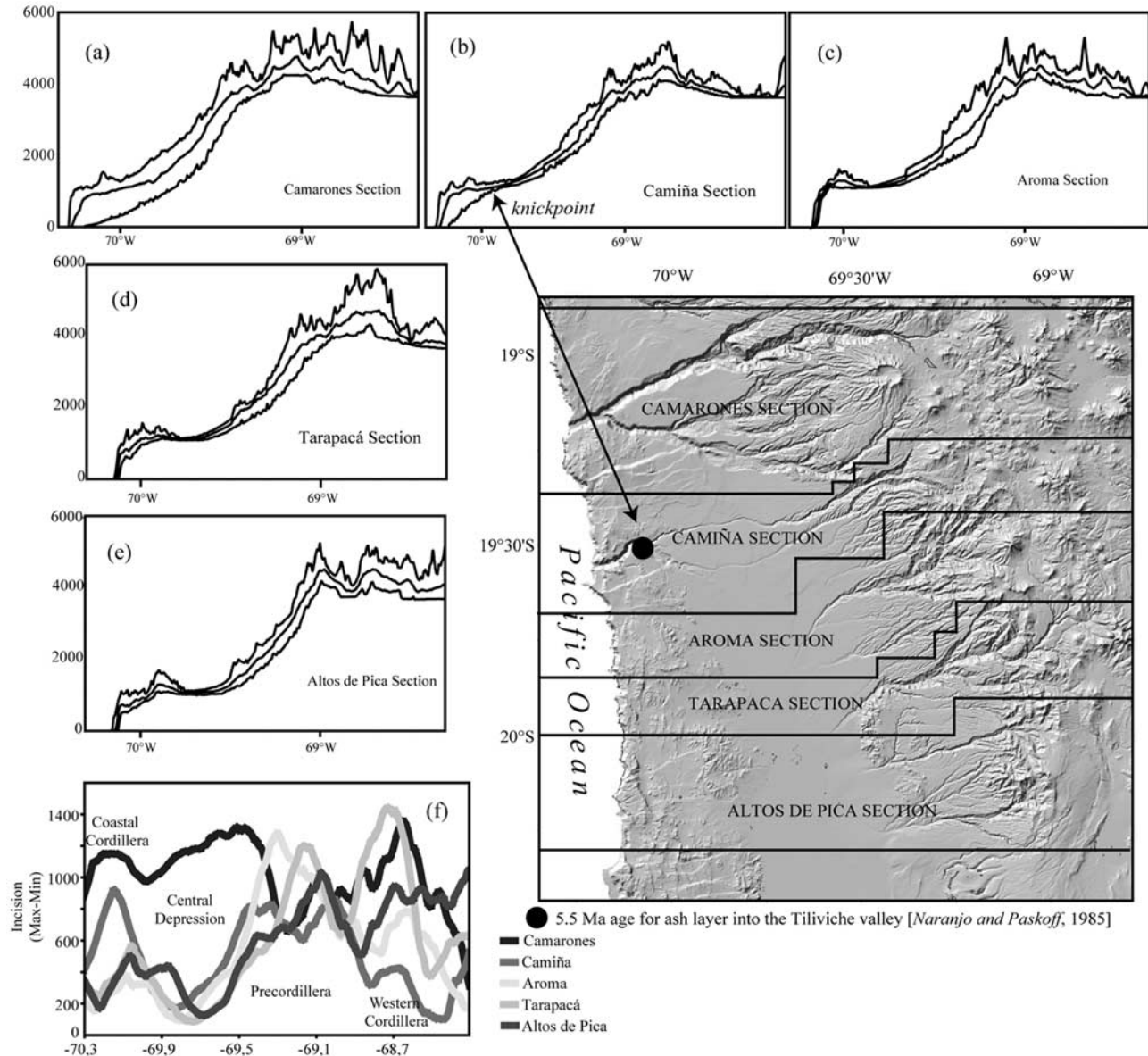


Figure 16. (a–e) W-E topographic profiles showing the minimum, mean, and maximum elevation for each section. (f) Comparison of incision level (maximum-minimum) for each section. It can be observed that the Camarones section and the Camiña section display a greater incision level in the Coastal Cordillera than other sections located into the endorheic zone. Nevertheless, the incision in the Precordillera is similar for all sections. The Camiña section exhibits a knickpoint resulting from the superposition of valley formation related to the seaward drainage opening over the erosion in the Precordillera. This proves that incision in the Precordillera does not result from the opening of the hydrologic system to the Pacific Ocean in that valley.

Pacific coast to the east through the Camiña and Tiliviche valleys (Figure 16). Therefore the 5.5 ± 0.6 Ma age would mark the older age for the beginning of incision related the drainage opening, at least in this valley. These dates confirm that the westward tilting had begun after 8 Ma, that is, when the shortening accommodated by the WTS slowed down. They also suggest that the change in the tectonic behavior of the North Chilean forearc was contemporaneous with the shift of the shortening from the

Eastern Cordillera to the sub-Andean Zone [Victor *et al.*, 2004].

5.3. Contribution of the Precordillera Flexure System and Westward Tilting to the Surface Uplift of the Western Flank of the Altiplano

[58] The ~ 2000 m relative surface uplift associated to the flexure system studied here is greater than that observed

north of the Aroma region [García, 2002; Pinto *et al.*, 2004], but slightly smaller than that observed to the south, in the Altos de Pica region [Victor *et al.*, 2004]. The surface elevation of the western flank of the Altiplano is almost constant along northern Chile, suggesting that the uplift related to the activity of the WTS could be underestimated in some places where the Cenozoic cover and its deformation are not well exposed [Pinto *et al.*, 2004].

[59] For estimating the contribution of the west vergent contractional structures on the surface uplift of the Chilean western side of the Altiplano, is necessary to take into account the paleoelevation and the paleorelief of the forearc before the beginning of the late Cenozoic uplift.

[60] In southernmost Peru, Tosdal *et al.* [1984] indicated that the Coastal Cordillera and Central Depression were close to the sea level during the Oligocene. The unconformity between the late Cenozoic series and the substratum (the “Choja Pediplain” of Galli [1967]) in the Precordillera and Central Depression of northern Chile can be considered, according to our observations, the observations by Galli [1967] and Tosdal *et al.* [1984], as well as the seismic profile shown by Victor *et al.* [2004], as a rather flat surface, even though there are some areas where the unconformity presents some irregularities that would correspond to local valley development during lower Oligocene times [Tosdal *et al.*, 1984; Fariás *et al.*, 2003]. The present-day elevation of this unconformity is not well constrained. Drill wells cut in the Central Depression indicate that the Mesozoic-late Cenozoic unconformity is located between 500 and 300 m asl; however, these wells were made in places where seismic reflection data detected topographic highs probably related to substratum structures [Mordojovich, 1965]. The seismic profile published by Victor *et al.* [2004] reveals that this unconformity in the Central Depression, west of the Altos de Pica region is located between 0 and 500 m asl. In this way, we can consider that this unconformity in the Central Depression and Precordillera underwent a 0–500 m of surface uplift since the Oligocene.

[61] In the Western Cordillera at the Arica region, Charrier *et al.* [1994], using the palinologic and paleobotanic content of the Chucal Formation as a paleoclimatic tool, estimated that this formation was deposited under paleoecological conditions controlled by a mean altitude of 1000 ± 200 m asl, whereas its present-day altitude is about 4200 m asl. Muñoz and Charrier [1996] indicate that the 3200 ± 200 m of surface uplift were registered before 4.8 Ma.

[62] In this way, we can consider that the surface over which the late Cenozoic series deposited corresponded to an almost unincised surface close to the sea level in the Coastal Cordillera reaching roughly to 1000 m asl in the Western Cordillera.

[63] Therefore we estimate that the Western Cordillera underwent a surface uplift of 2500–3400 m with respect to the Central Depression during the late Cenozoic. Considering that the WTS in the Aroma region accommodates about 2000 m of this uplift, then the remaining 500–1400 m should have been accommodated by other processes. We propose that this remaining 500–1400 m of relative surface

uplift resulted from the westward tilting of the forearc. The incision observed in the Precordillera of the Camiña and Aroma region (600–800 m) is within this range, providing more evidences for the link between incision and tilting. If the tilting extends from the Central Depression to the Western Cordillera, then it should be necessary about 1° to accommodate 1 km of relative uplift. Several hundreds of kilometers to the south, in the southern Atacama desert ($26\text{--}27^\circ\text{S}$), Riquelme [2003] also propose a post-10 Ma westward tilting of about 1° for explaining the incision of the Precordillera: Analyzing pre-Miocene river valley profiles, Riquelme [2003] showed that the tilting has been smaller than the value of 3° suggested by Lamb *et al.* [1997]. In fact, if we consider a 80-km-long tilted zone (approximate distance between the western Central Depression and the Western Cordillera according to the length of the west dipping seismological structure observed by David *et al.* [2002] and Comte *et al.* [2003a]), then 3° of tilting would result in more than 4000 m of relative surface uplift of the Western Cordillera, which is too much, taking into account the relative uplift accommodated by the WTS.

5.4. Pliocene-Recent Strike-Slip Motion and Strain Partitioning

[64] The crustal strain related to the seismic activity registered in 2001 and 2002 in the Aroma region differs from that accumulated on the WTS during Oligocene-Neogene times, even though the Aroma earthquake would have occurred along the same fault that propagates upward as the Aroma flexure. In the Altos de Pica region, Victor *et al.* [2004] found evidences of N-S strike-slip motion and pull-apart basin formation with NW-SE extension bordering the Salar de Huasco, which would have begun in the late Pliocene. Although we did not find either geological or geomorphological evidence of surface deformation related to strike-slip motion around the zone where the seismic activity took place, the focal mechanisms of the Aroma and Chusmiza earthquakes correlate with the strike-slip deformation observed in the Altos de Pica region, which could represent the present-day crustal state of that part of the Precordillera (Figure 17).

[65] In contrast, north of Aroma, David *et al.* [2002] revealed that the deep forearc of the Arica region ($18^\circ\text{--}19^\circ\text{S}$) undergoes ENE-WSW shortening associated with the activity of east vergent thrusts (Figure 17). The p axis mechanism of the Aroma earthquake, the Pliocene-Recent σ_1 direction estimated in the Altos de Pica [Victor *et al.*, 2004], and the maximum stress axis calculated by David *et al.* [2002] in the Arica region are almost parallel to the present-day plate convergence direction (Figure 17).

[66] Compressive active tectonic regime is observed north of the change in the trend of the Precordillera structures ($\sim 19^\circ 30'\text{S}$), while strike slip is observed to the south. In this case, transition from strike-slip to thrust-slip faults could result from the different obliquity of the structures with respect to the plate convergence direction: North of the Aroma region, structures are almost orthogonal to the convergence, favoring ENE-WSW shortening; south

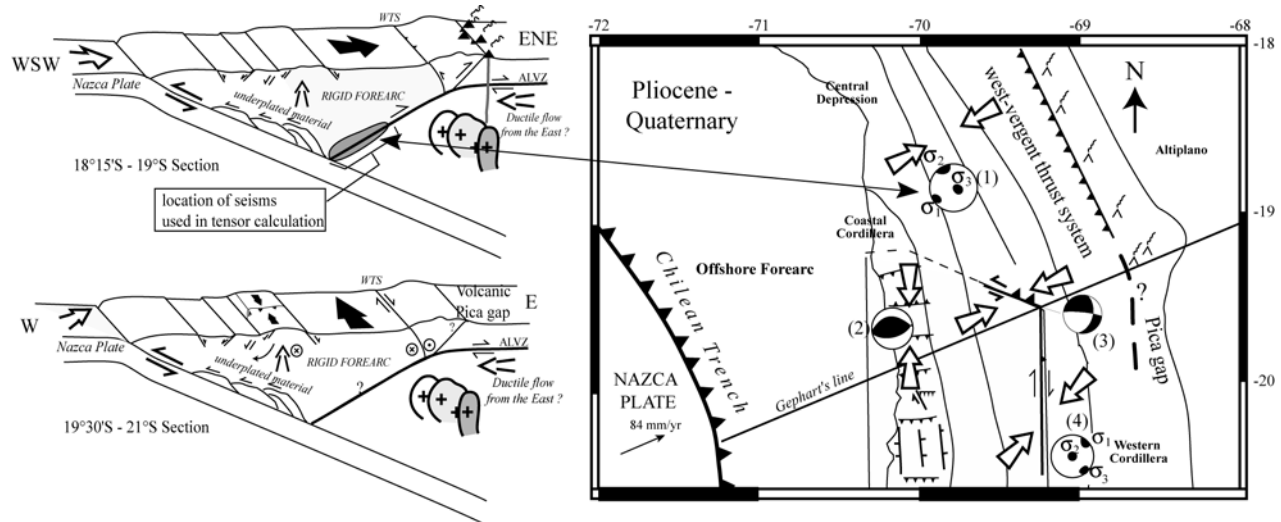


Figure 17. Present-day tectonic regime of the western flank of the Altiplano in northern Chile. The stress tensor calculated north of 19°S (1) was determined by *David et al.* [2002] based on the crustal seismicity located between 30 and 60 km depth. On the basis of the kinematic analysis of E-W thrusts located in the Coastal Cordillera, *Allmendinger et al.* [2005] determined N-S shortening (2). In the eastern side of the Precordillera in the Altos de Pica region, *Victor et al.* [2004] found evidences of N-S dextral motion and pull-apart development with an NW-SE extension (4). The focal mechanisms determined by the Harvard CMT for the Aroma and Chusmiza earthquakes (3) show an equivalent strain regime as the Altos de Pica region.

of 19°30'S, in contrast, structures are slightly oblique to the convergence, and strike-slip faulting occurs (Figure 17). The stress regime observed by *David et al.* [2002] may also, however, reflect the horizontal shortening prevailing in the lower crust, while the strike slip could correspond to superficial deformation.

[67] The Coastal Cordillera between 19°S and 21°30'S is the highest segment of this range in northern Chile. Along this belt, extensional deformation is documented by ~N-S normal faults [e.g., *González et al.*, 2003] (see Figure 17). Similar active normal faults are observed along the whole Chilean coast, especially where the distance between the coast and the trench is small, suggesting they are the consequence of crustal underplating resulting from the Nazca plate subduction [e.g., *Adam and Reuther*, 2000; *Delouis et al.*, 1998; *Ortlieb et al.*, 1996]. On the other hand, several ~E-W thrusts accommodated about 3 km of shortening between the Camarones and Loa river valleys (19°–21°15'S) since the latest Miocene [*Allmendinger et al.* [2005] (Figure 17). In the Precordillera, the Soga fault (~19°25'S) also accommodates NNE-SSW shortening and ESE-WNW sinistral strike-slip motion, a few kilometers north of the changing trend of the Precordilleran structures. Furthermore, between the same latitudes, the Central Depression exhibits a southward tilting (Figure 6), which would have begun after 7 Ma.

[68] The strain partitioning observed in the forearc between 19°S and 21°30'S could reflect the particular rigid rheology of the crustal forearc and its strong coupling within the interplate zone, the obliquity of the plate convergence direction and the geometry of the plate boundary.

There, the continental margin is concave toward the subducting plate, what should facilitate the N-S shortening due to a “buttress effect” [*Beck*, 1991]; south of *Gephart's* [1994] symmetry plane, the forearc would be displaced to the north as a result of the oblique convergence of the Nazca and South America plates (Figure 17, see also the model of *Bevis et al.* [2001]). This motion would explain the N-S shortening observed in the Coastal Cordillera and the strike-slip deformation affecting the Precordillera (Figure 17).

[69] Similar strain partitioning is observed in the southern central Andes forearc (~37°S–42°S) where the Central Depression exhibits ~N-S shortening and the intra-arc zone is dominated by transpressive N-S strike-slip motion along the Liquiñe-Ofqui fault zone, where the continental margin is also concave toward the ocean [*Lavenue and Cembrano*, 1999].

5.5. Geodynamic Evolution and Origin of the Uplift in the Western Side of the Altiplano

[70] The uplift accommodated by the WTS cannot be explained as an isolate process due to the small shortening registered in the western Altiplano. *Victor et al.* [2004] observe that the surface uplift of the Western Cordillera with respect to the Central Depression did not result in significant tectonic subsidence of the forearc, and they conclude that the relative uplift of the Western Cordillera must have been accompanied by crustal thickening under that part of the central Andes. The maximum relative uplift rates that occurred between the late Oligocene and the middle Miocene along the Precordillera were coeval with the produc-

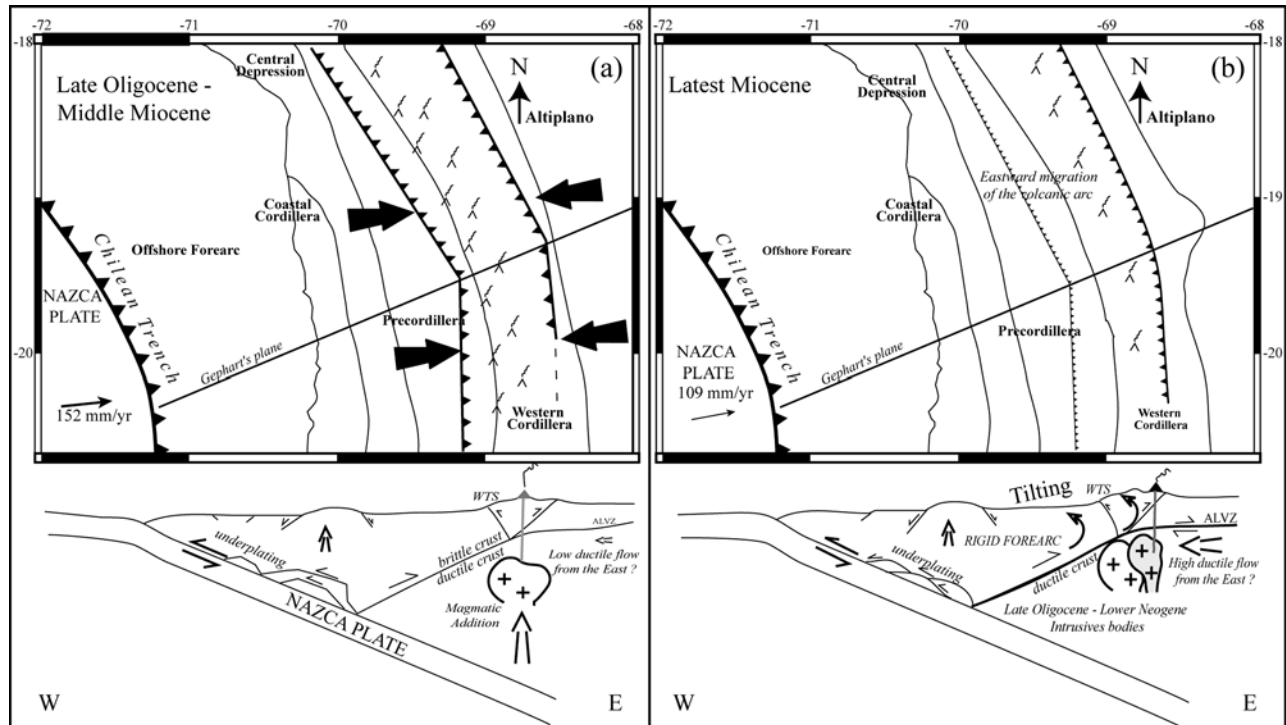


Figure 18. Schematic evolution of the uplift of the western side of the Altiplano in northern Chile. (a) Tectonic situation between 26 and 8 Ma, where rapid and orthogonal plate convergence was the main tectonic feature. During this time, large volumes of magma were emplaced below the Precordillera and Western Cordillera. Little ductile flow of the lower crust is expected for this time. (b) Tectonic situation in the latest Miocene. At this time, nearly 1–3 km of surface uplift occurred within the Altiplano as a result of crustal thickening, probably triggered by the hypothetical ductile flow of the lower crust coming from the sub-Andean zone to the Altiplano. This uplift is marked by westward forearc tilting. Morphologic units (trench, coastline, Coastal Cordillera, Central Depression, Precordillera, and Western Cordillera) are reported in their present-day location. Plate convergence vector is after Somoza [1998].

tion of great volumes of magma in the present-day forearc and large rate of shortening in the eastern Altiplano [Gubbels et al., 1993; Hérail et al., 1996; Lamb and Hoke, 1997; Lamb et al., 1997; Sempere et al., 1990] (Figure 18a). In this way, the activity of the WTS could correspond to the upper crustal tectonic accommodation of these two processes that may have resulted in crustal thickening below the central Andes.

[71] During the late Oligocene and Neogene, before 8 Ma, the deformation of the here studied system of flexures resulted in almost 2 km of surface uplift of the Western Cordillera with respect to the Central Depression. It is probable that during that period most of the relative uplift of the Western Cordillera was accommodated by the WTS (Figure 18a). As previously mentioned, during the same period, thrust faults were active on the eastern side of the Western Cordillera (Figure 18a), within the Altiplano and the Eastern Cordillera. However, crustal shortening within the Altiplano was not intense enough to explain the present-day Moho depth and topographic altitude of the high plateau [e.g., Husson and Sempere, 2003]. Gregory-Wodzicki [2000] notes, indeed, that the altitude of the high plateau was significantly lower than the present-day elevation 10 Myr ago, although this epoch marks the end of the

compressive tectonic activity at the surface of the plateau and it shift to the sub-Andean zone [e.g., Gregory-Wodzicki, 2000; Gubbels et al., 1993].

[72] In fact, crustal thickening resulting from the tectonic shortening and/or magmatic accretion warms up and hence diminishes the viscosity of the lower crust. Lower viscosity, in turn, facilitates the development of lateral ductile fluxes within lower crustal levels that homogenizes the thickness of the crust below the orogen and result in the formation of high plateau [Bird, 1991; Husson and Sempere, 2003]. This process may explain why, although most of the superficial crustal shortening accommodated within the central Andes from circa 10 Ma concentrated in the sub-Andean ranges [Gubbels et al., 1993], underthrusting of the Brazilian Craton resulted in a general surface uplift of the entire width of the orogen. Indeed, the direct link of the ALVZ to the basal detachment under the eastern flank of the Altiplano probably separating crustal shortening in an upper crust imbricate belt from a mechanically weakened deeper crust [Yuan et al., 2000] supports the tectonic relevance of the presence of mechanically decoupled zones within the crust during the central Andes plateau development. Following Lamb et al. [1997] or Husson and Sempere [2003], we think that the tremendous late Neogene uplift reported

for the Altiplano by *Gregory-Wodzicki* [2000] resulted from a huge deep ductile mass transfer that may also have contributed, in a minor amount, to an additional uplift of the Western Cordillera. *Tassara* [2005] suggests that the high rigidity of the forearc region, resulting from the thermomechanical coupling with the cold subducted slab, forces this lower crustal flow coming from the east to be accumulated below the Altiplano, the Western Cordillera and the west dipping plane below the forearc. This process should be responsible for the westward tilting of the western flank of the Altiplano observed in northern Chile and that, moreover, was coeval with the huge surface uplift of the plateau.

[73] To conclude, we suggest that the late Oligocene-Neogene tectonic evolution of the forearc around the Aroma region has been split into two periods: (1) the beginning of the underthrusting of the Brazilian Craton below the sub-Andean zone coincided with the end of surface shortening within the Altiplano, the Eastern Cordillera and the Western Cordillera. It marked the end of the rapid relative uplift accommodated by the WTS (Figure 18a); and (2) the further surface uplift of the Western Cordillera could be explained as a result of deep crustal ductile mass transfer and/or magmatic accretion, and it would have been essentially accommodated in the surface by the subtle tilting of a wide part of the forearc (Figure 18b). Meanwhile, the tectonic regime accommodated by the WTS changed to become essentially transcurrent (Figure 17), which may be as a result of the increasing elevation of the region which would oppose horizontal shortening [e.g., *Dalmayrac and Molnar*, 1981], as well as the increase in the obliquity of the plate convergence vector since the Pliocene [*Somoza*, 1998].

6. Conclusions

[74] Since late Oligocene times, the western flank of Altiplano in northern Chile underwent important surface uplift related to contractional strain, which was mainly accommodated by west vergent thrusts propagating into west dipping monocline folds (flexures). During the growth of folding, large amount of ignimbrites and coarse conglomerates were emplaced above a major erosional sub-planar surface developed during Oligocene that *Galli's* [1967] early work already described as "The Choja Pediplain". These syntectonic deposits were progressively deformed by the growing flexures, forming spectacular growth strata that allow us to determine amounts and rates of relative uplift. Although we considered the 26 Ma age as the beginning of the activity along the flexures, the onset of deformation could be as old as ~30 Ma, according to the studies of *Sempere et al.* [1990], *García* [2002] and *Victor et al.* [2004]. Since then, ~2 km of relative surface uplift has been accommodated by the WTS in the studied region.

[75] On the basis of seismological, geophysical and geological works, we suggest that the structural configuration of the western flank of the Altiplano in northern Chile, at least between 18°S and 21°S, corresponds to a crustal-scale fault bend fold, consisting of a main west dipping ramp extended from the Wadati-Benioff zone beneath the Coastal Cordillera to the Western Cordillera, continuing as a

flat discontinuity farther east below the Altiplano (ALVZ). On the tip of the ramp, at 20–30 km depth, both west and east vergent thrusts emerge to the surface, accommodating the uplift in the upper brittle crust.

[76] We can separate the evolution of the western flank of the Altiplano into two periods:

[77] 1. The major relative surface uplift occurred between late Oligocene and middle Miocene (26–8 Ma) at a rapid uplift rate of ~0.10 mm/yr, coeval with volcanic activity in the Precordillera, widely distributed conglomerate deposition on the forearc, a large rate of shortening within the Altiplano and Eastern Cordillera, and rapid and normal plate convergence. As observed by *Victor et al.* [2004], the relative uplift of the Western Cordillera did not result in significant subsidence of the forearc, which means that the uplift was accompanied by crustal thickening due to tectonic shortening and magmatic addition.

[78] 2. Since 8 Ma, the uplift rates related to the WTS diminished to 0.02 mm/yr. At this time, the volcanic activity shifted from the Precordillera to its present-day location in the Western Cordillera, hyperarid condition settles along the forearc of northern Chile, and started the incision in the Precordillera related to westward tilting of the forearc. Tilting contributed 500–1000 m to the surface uplift. Meanwhile, the WTS, at least south of 19°20'S, accommodated N-S dextral strike-slip motion, while along the Coastal Cordillera, between 19° and 21°30'S, about 3 km of N-S shortening occurs [*Allmendinger et al.*, 2005].

[79] After 10 Ma and the shifting of active shortening from the plateau and Eastern Cordillera to the sub-Andean zone, the whole Altiplano underwent 1–3 km of surface uplift. This uplift probably resulted partly from crustal thickening triggered by the underthrusting of the Brazilian Craton below the sub-Andean zone and the increase of a proposed lateral ductile flow within the lower crust that would homogenize the crustal thickness on the entire Altiplano. Following the models of *Lamb et al.* [1997], we argue that this flow would be the responsible for the westward forearc tilting, which occurred during this time.

[80] The transurrence and strain partitioning that now prevail along the forearc between 19° and 21°30'S would be the consequence of an increase in the obliquity of the plate convergence vector since the Pliocene [*Somoza*, 1998], favored by the rigid forearc rheology, strong coupling of the interplate zone, "buttress effect" due to the westward concavity of the continental margin and WTS around the *Gephart's* [1994] symmetric plane of the central Andes, as well as the high elevation of the region that opposes horizontal shortening.

[81] **Acknowledgments.** This study was funded partially by grant FONDECYT 1020104 to Diana Comte and the Institut de Recherche pour le Développement (IRD, France). This research is part of the international collaboration agreement between the Universidad de Chile (Departamento de Geología and Departamento de Geofísica) and the IRD. The authors wish to thank the following colleagues for valuable help during this work: César Arriagada, Laurence Audin, Claire David, Marcelo García, Muriel Gerbault, Mario Pardo, Luisa Pinto, Rodrigo Riquelme, Pierrick Roperch, and Andrés Tassara. Special thanks to Mark Jessel for improving the English text. This article was greatly improved by the diligent reviews of Onno Oncken, Fritz Schlunegger, Simon Lamb, and Barbara Carrapa.

References

- Adam, J., and C.-D. Reuther (2000), Crustal dynamics and active fault mechanics during subduction erosion. Application of frictional wedge analysis on to the North Chilean Forearc, *Tectonophysics*, **321**, 297–325.
- Allmendinger, R. W., T. E. Jordan, S. M. Kay, and B. Isacks (1997), The evolution of the Altiplano-Puna Plateau of the central Andes, *Annu. Rev. Earth Planet. Sci.*, **25**, 139–174.
- Allmendinger, R. W., G. González, J. Yu, G. Hoke, and B. Isacks (2005), Trench-parallel shortening in the northern Chilean Forearc: Tectonic and climatic implications, *Geol. Soc. Am. Bull.*, **117**, 89–104.
- Ameen, M. S. (1988), Forced folding of layered cover due to dip-slip, basement faulting, Ph.D. thesis, Univ. of London, London.
- ANCORP Working Group (1999), Seismic reflection image revealing offset of Andean subduction-zone earthquake locations into oceanic mantle, *Nature*, **397**, 341–345.
- ANCORP Working Group (2003), Seismic imaging of a convergent continental margin and plateau in the Central Andes (Andean Continental Research Project 1996 (ANCORP'96)), *J. Geophys. Res.*, **108**(B7), 2328, doi:10.1029/2002JB001771.
- Baby, P., P. Rochat, G. Mascle, and G. Hérail (1997), Neogene shortening contribution to crustal thickening in the back arc system of the Bolivian Orocline (central Andes), *Geology*, **25**, 883–886.
- Beck, M. S. (1991), Coastal transport reconsidered: Lateral displacements in oblique subduction zones, and tectonic consequences, *Phys. Earth Planet. Inter.*, **68**, 1–8.
- Beck, S. L., and G. Zandt (2002), The nature of orogenic crust in central Andes, *J. Geophys. Res.*, **107**(B10), 2230, doi:10.1029/2000JB000124.
- Bevis, M., E. Kendrick, R. Smalley Jr., B. Brooks, R. Allmendinger, and B. Isacks (2001), On the strength of interplate coupling and the rate of back arc convergence in the central Andes: An analysis of the interseismic velocity field, *Geochim. Geophys. Res.*, **2**(11), doi:10.1029/2001GC000198.
- Bird, P. (1991), Lateral extrusion of lower crust from under high topography in isostatic limit, *J. Geophys. Res.*, **96**, 10,275–10,286.
- Burbank, D., and R. S. Anderson (2001), *Tectonic Geomorphology*, 274 pp., Blackwell Sci., Malden, Mass.
- Burbank, D., and J. Vergés (1994), Reconstruction of topography and related depositional systems during active thrusting, *J. Geophys. Res.*, **99**, 20,281–20,297.
- Charrier, R., N. Muñoz, and S. Palma-Heldt (1994), Edad y contenido paleoflorístico de la Formación Chuca y condiciones paleoclimáticas para el Oligoceno Tardío-Mioceno Inferior en el Altiplano de Arica, Chile, paper presented at 7th Congreso Geológico Chileno, Dep. de Cienc. de la Tierra, Univ. de Concepción, Concepción, Chile.
- Charrier, R., G. Hérail, J. J. Flynn, R. Riquelme, M. García, D. Crift, and A. Wyss (1999), Opposite thrust-vergencies in the Precordillera and Western Cordillera in northern Chile and structural linked Cenozoic paleoenvironmental evolution, paper presented at 4th International Symposium on Andean Geodynamics, Inst. Fr. de Rech. Sci. pour le Dev. en Coop. (ORSTOM), Göttingen, Germany.
- Charrier, R., G. Hérail, J. J. Flynn, R. Riquelme, M. García, D. Croft, and A. Wyss (2000), El Cordón Chapiquiña-Belén en el borde occidental del Altiplano chileno: Significado paleogeográfico y contexto tectónico regional, paper presented at 9th Congreso Geológico Chileno, Serv. Nac. de Geol. y Miner., Puerto Varas, Chile.
- Charrier, R., A. Chávez, S. Elgueta, G. Hérail, J. J. Flynn, D. Croft, A. Wyss, and M. García (2002), Rapid tectonic and paleogeographic evolution: The Chuca Anticline, Altiplano de Arica, northern Chile, paper presented at 5th International Symposium on Andean Geodynamics, Inst. de Rech. Sci. pour le Dev. en Coop. (IRD), Toulouse, France.
- Coira, B., J. Davidson, C. Mpodozis, and V. Ramos (1982), Tectonic and magmatic evolution of the Andes of northern Argentina and Chile, *Earth Sci. Rev.*, **18**, 303–332.
- Comte, D., and M. Pardo (1991), Reappraisal of the great historical earthquake in the northern Chile and southern Peru seismic gaps, *Nat. Hazard*, **4**, 23–44.
- Comte, D., et al. (2001), Analysis of the 24 July 2001 shallow earthquake $M_w = 6.3$ recorded in the northern Chile Altiplano, *Eos Trans. AGU*, **82**(47), Fall Meet. Suppl., Abstract S52A-0616.
- Comte, D., C. Dorbath, R. Boroscchek, L. Dorbath, B. Glass, E. Correa, C. Meneses, A. Cruz, H. Haessler, and M. Frogneux (2002), Shallow seismicity around the Arica bend in western Altiplano piedmont, *Eos Trans. AGU*, **83**(47), Fall Meet. Suppl., Abstract S71C-1112.
- Comte, D., C. Dorbath, L. Dorbath, M. Fariás, C. David, H. Haessler, B. Glass, E. Correa, I. Balmaceda, A. Cruz, and L. Ruz (2003a), Distribución temporal y en profundidad de la réplicas del sismo superficial de Arica, Norte de Chile del 24 de Julio de 2001, paper presented at 10th Congreso Geológico Chileno, Univ. de Concepción, Concepción, Chile, 6–10 Oct.
- Comte, D., H. Tavera, C. David, D. Legrand, L. Dorbath, A. Gallego, J. Pérez, H. Haessler, E. Correa, and A. Cruz (2003b), Seismotectonic characteristics around the Arica bend, central Andes (16°S–20°S): Preliminary results, *Eos Trans. AGU*, **84**(46), Fall Meet. Suppl., Abstract S41A-05.
- Dalmayrac, B., and P. Molnar (1981), Parallel thrust and normal faulting in Peru and constraints on the state of stress, *Earth Planet. Sci. Lett.*, **55**, 473–481.
- David, C., J. Martinod, D. Comte, G. Hérail, and H. Haessler (2002), Intracontinental seismicity and Neogene deformation of the Andean forearc in the region of Arica (18.5°S–19.5°S), paper presented at 5th International Symposium on Andean Geodynamics, Inst. de Rech. pour le Dev. (IRD), Toulouse, France.
- Delouis, B., H. Phillip, L. Dorbath, and A. Cisternas (1998), Recent crustal deformation in the Antofagasta region (northern Chile) and the subduction process, *Geophys. J. Int.*, **132**, 302–338.
- DeMets, C., R. Gordon, F. Argus, and S. Stein (1994), Current plate motions, *Geophys. J. Int.*, **101**, 425–478.
- Dingman, R. J., and C. Galli (1965), Geology and ground-water resources of the Pica area, Tarapaca Province, Chile, *U.S. Geol. Surv. Bull.*, **1189**, 113 pp.
- Dorbath, C., and F. Masson (2000), Composition of the crust and upper-mantle in the central Andes (19°30'S) inferred from P wave velocity and Poisson's ratio, *Tectonophysics*, **327**, 213–223.
- Fariás, M. (2003), Evolución morfo-tectónica cenozoica y la sismicidad superficial del piedemonte altiplánico chileno entre los 19°25'S–19°45'S, thesis, Dep. de Geol., Univ. de Chile, Santiago.
- Fariás, M., R. Charrier, D. Comte, J. Martinod, L. Pinto, and G. Hérail (2002), Active Late Cenozoic flexures in the Precordillera in northern Chile: Correlations with the shallow seismic activity, and implications for the uplift of the Altiplano, *Eos Trans. AGU*, **83**(47), Fall Meet. Suppl., Abstract T51A-1136.
- Fariás, M., R. Charrier, J. Martinod, D. Comte, and G. Hérail (2003), Interacción de los mecanismos de erosión, sedimentación, volcanismo y tectónica en el desarrollo morfológico del piedemonte altiplánico en la Región de Tarapacá durante el Cenozoico Superior, paper presented at 10th Congreso Geológico Chileno, Univ. de Concepción, Concepción, Chile, 6–10 Oct.
- Ford, M., E. Williams, and A. Artori (1997), Progressive evolution of a fault-related fold pair from growth strata geometries, Sant Llorenç de Morunys SE Pyrenees, *J. Struct. Geol.*, **19**, 413–441.
- Galli, C. (1957), Las formaciones geológicas en el borde occidental de la Puna de Atacama, sector de Pica, Tarapacá, *Minerales*, **12**, 14–26.
- Galli, C. (1967), Piediplain in northern Chile and the Andean uplift, *Science*, **158**, 653–655.
- Galli, C., and I. Dingman (1962), Cuadrángulos Pica, Alca, Matilla y Chacarilla, con un estudio sobre los recursos de agua subterránea, Provincia de Tarapacá, *Carta Geol. Chile*, **3**, 125 pp.
- Gansser, A. (1973), Facts and theories on the Andes, *J. Geol. Soc. London*, **129**, 93–131.
- García, M. (1996), Geología y estructura del borde del Altiplano occidental, en el área de Belén (Chile), thesis, Dep. de Geol., Univ. de Chile, Santiago.
- García, M. (2002), Évolution oligo-néogène de l'Altiplano Occidental (Arc et Avant-Arc du Nord du Chili, Arica): Tectonique, volcanisme, sédimentation, géomorphologie et bilan érosion-sédimentation, Ph.D. thesis, Univ. Joseph Fourier, Grenoble, France.
- García, M., and G. Hérail (2001), Comment on 'Geochronology (Ar-Ar, K-Ar and He-exposure ages) of Cenozoic magmatic rocks from northern Chile (18–22°S): Implications for magmatism and tectonic evolution of the central Andes' of Wörner et al. (2000), *Rev. Geol. Chile*, **28**, 127–130.
- García, M., G. Hérail, and R. Charrier (1996), The Cenozoic forearc evolution in Northern Chile: The western border of the Altiplano de Belén (Chile), paper presented at 3rd International Symposium on Andean Geodynamics, Inst. Fr. de Rech. Sci. pour le Dev. en Coop. (ORSTOM), Saint Malo, France.
- García, M., G. Hérail, and R. Charrier (1999), Age and structure of the Oxaya antiline: A major feature of the Miocene compressive structure of northernmost Chile, paper presented at 4th International Symposium on Andean Geodynamics, Inst. Fr. de Rech. Sci. pour le Dev. en Coop. (ORSTOM), Göttingen, Germany.
- García, M., G. Hérail, R. Charrier, G. Mascle, M. Fornari, and C. Pérez de Arce (2002), Oligocene-Neogene tectonic evolution of the Altiplano de northern Chile (18–19°S), paper presented at 5th International Symposium on Andean Geodynamics, Inst. de Rech. pour le Dev. (IRD), Toulouse, France.
- Gaupp, R., A. Kött, and G. Wörner (1999), Palaeoclimatic implications of Mio-Pliocene sedimentation in the high-altitude intra-arc Lauca Basin of northern Chile, *Palaeogeogr. Palaeoclimatol. Palaeoecol.*, **151**, 79–100.
- Gephart, J. W. (1994), Topography and subduction geometry in the Central Andes: Clues to the mechanics of a non-collisional orogen, *J. Geophys. Res.*, **99**, 12,279–12,288.
- Gerbault, M., G. Hérail, and J. Martinod (2002), Numerical modelling of deformation processes in the Andes, paper presented at 5th International Symposium on Andean Geodynamics, Inst. de Rech. pour le Dev. (IRD), Toulouse, France.
- Gill, J. B. (1981), *Orogenic Andesites and Plate Tectonics*, 390 pp., Springer, New York.
- González, G., J. Cembrano, D. Carrizo, A. Macci, and H. Schneider (2003), The link between forearc tectonics and Pliocene-Quaternary deformation of the Coastal Cordillera, northern Chile, *J. S. Am. Earth Sci.*, **16**, 321–342.
- Gregory-Wodzicki, K. (2000), Uplift history of central and northern Andes: A review, *Geol. Soc. Am. Bull.*, **112**, 1091–1105.
- Gregory-Wodzicki, K., W. C. Macintosh, and K. Velázquez (1998), Climatic and tectonic implications of the late Miocene Jakokhota flora, Bolivian Altiplano, *J. S. Am. Earth Sci.*, **11**, 533–560.

- Gubbels, T., B. Isacks, and E. Farrar (1993), High-level surfaces, plateau uplift and foreland development, Bolivian central Andes, *Geology*, **21**, 695–698.
- Haessler, H., et al. (2000), Shallow seismicity beneath the Altiplano piedmont, northern Chile: Preliminary results, *Eos Trans. AGU*, **81**(48), Fall Meet. Suppl., Abstract S21A-07.
- Harambour, S. (1990), Geología pre-cenozoica de la Cordillera de los Andes entre las quebradas Aroma y Juan de Morales, I Región, thesis, Dep. de Geol., Univ. de Chile, Santiago.
- Haschke, A., and A. Günther (2003), Balancing crustal thickening in arcs by tectonic vs. magmatic means, *Geology*, **31**, 933–936.
- Hérail, G., J. Oller, P. Baby, M. Bonhomme, and P. Soler (1996), Strike-slip faulting, thrusting and related basin in the Cenozoic evolution of the southern branch of the Bolivian Orocline, *Tectonophysics*, **259**, 201–212.
- Hoke, L., D. Hilton, S. Lamb, K. Hammerschmidt, and H. Friedrichson (1994), ³He evidence for a wide zone of active mantle melting beneath the central Andes, *Earth Planet. Sci. Lett.*, **128**, 341–355.
- Husson, L., and T. Sempere (2003), Thickening the Altiplano crust by gravity-driven crustal channel flow, *Geophys. Res. Lett.*, **30**(5), 1243, doi:10.1029/2002GL016877.
- Isacks, B. L. (1988), Uplift of the central Andean plateau and bending of the Bolivian Orocline, *J. Geophys. Res.*, **93**, 3211–3231.
- Jordan, T. E., B. L. Isacks, R. W. Allmendinger, J. A. Brewer, V. Ramos, and C. J. Ando (1983), Andean tectonics related to geometry of subducted Nazca plate, *Geol. Soc. Am. Bull.*, **94**, 341–361.
- Kay, S., and J. M. Abbruzzi (1996), Magmatic evidence for Neogene lithospheric evolution of the central Andes “flat-slab” between 30°S and 32°S, *Tectonophysics*, **259**, 15–28.
- Kay, S. M., C. Mpodozis, V. A. Ramos, and F. Munizaga (1991), Magma source variations for mid-late Tertiary magmatic rocks associated with a shallowing subduction zone and a thickening crust in the central Andes (28 to 33°S), *Spec. Pap. Geol. Soc. Am.*, **265**, 113–137.
- Kay, S. M., C. Mpodozis, and B. Coira (1999), Neogene magmatism, tectonics, and mineral deposits of the central Andes (22 to 33°S), in *Geology and Ore Deposits of the Central Andes*, edited by B. J. Skinner, *Spec. Publ. SEPM Soc. Sediment. Geol.*, **7**, 27–59.
- Kiefer, E., M. J. Dorr, H. Ibbeken, and H.-J. Götze (1997), Gravity-based mass balance of an alluvial fan giant: The Arcas Fan, Pampa del Tamarugal, northern Chile, *Rev. Geol. Chile*, **24**, 165–185.
- Kley, J., and C. R. Monaldi (1998), Tectonic shortening and crustal thickness in the central Andes: How good is the correlation?, *Geology*, **26**, 723–726.
- Kley, J., C. R. Monaldi, and J. A. Salfity (1997), Along-strike segmentation of the Andean foreland: Causes and consequences, *Tectonophysics*, **301**, 75–94.
- Kono, M., Y. Fukao, and A. Yamamoto (1989), Mountain building in the central Andes, *J. Geophys. Res.*, **94**, 3891–3905.
- Kött, A., R. Gaupp, and G. Wörner (1996), Miocene to recent history of the Western Altiplano in northern Chile revealed by lacustrine sediments of the Lauca Basin (18°15′/18°40′S–69°30′/69°05′W), *Geol. Rundsch.*, **84**, 770–780.
- Lamb, S., and L. Hoke (1997), Origin of the high plateau in the central Andes, Bolivia, South America, *Tectonics*, **16**, 623–649.
- Lamb, S., L. Hoke, L. Kennan, and J. Dewey (1997), Cenozoic evolution of the central Andes in Bolivia and northern Chile, in *Orogens Through Time*, edited by J.-P. Burg and M. Ford, *Geol. Soc. Spec. Publ.*, **121**, 237–264.
- Lavenu, A., and J. Cembrano (1999), Compressional- and transpressional-stress pattern for Pliocene and Quaternary brittle deformation in fore arc and intra-arc zones (Andes of central and southern Chile), *J. Struct. Geol.*, **21**, 1669–1691.
- Martinod, J., D. Comte, C. David, M. Vallée, G. Hérail, L. Audin, and M. Fariás (2002), Superficial crustal seismicity in northern Chile and the seismic cycle on the Nazca subduction zone, paper presented at EGS XXVI General Assembly, Eur. Geol. Soc., Nice, France.
- Masson, F., C. Dorbath, C. Martinez, and G. Carlier (2000), Local earthquake tomography of the Andes at 20°S: Implications for the structure and building of the mountain range, *J. S. Am. Earth Sci.*, **14**, 3–19.
- McQuarrie, N. (2002), The kinematic history of the central Andean fold-thrust belt, Bolivia: Implications for building a high plateau, *Geol. Soc. Am. Bull.*, **114**, 950–963.
- McQuarrie, N., and P. G. DeCelles (2001), Geometry and structural evolution of the central Andean back-thrust belt, Bolivia, *Tectonics*, **20**, 669–692.
- Miall, A. D. (1985), Architectural-element analysis: A new method of facies analysis applied to fluvial deposits, *Earth Sci. Rev.*, **22**, 261–308.
- Miall, A. D. (1996), *The Geology of Fluvial Deposits: Sedimentary Facies, Basin Analysis and Petroleum Geology*, 582 pp., Springer, New York.
- Montecinos, F. (1963), Observaciones de Geología en el Cuadrángulo Campanani, Departamento de Arica, thesis, Dep. de Geol., 109 pp., Univ. de Chile, Santiago.
- Mordojovich, C. (1965), Reseña sobre las exploraciones de la ENAP en la zona norte, años 1956 a 1962, *Minerales*, **20**, 30 pp.
- Mortimer, C. (1980), Drainage evolution in the Atacama Desert of northernmost Chile, *Rev. Geol. Chile*, **11**, 3–28.
- Mortimer, C., and N. Saric (1972), Landform evolution in the coastal region of Tarapaca Province, Chile, *Rev. Géomorphol. Dyn.*, **21**, 2, 162–170.
- Mortimer, C., and N. Saric (1975), Cenozoic studies in northernmost Chile, *Geol. Rundsch.*, **64**, 395–420.
- Mortimer, C., E. Farrar, and N. Saric (1974), K-Ar ages from Tertiary lavas of the northernmost Chilean Andes, *Geol. Rundsch.*, **63**, 395–420.
- Mpodozis, C., and V. Ramos (1989), The Andes of Chile and Argentina, in *Geology of the Andes and Its Relation to Hydrocarbon and Minerals Resources*, *Earth Sci. Ser.*, vol. 11, edited by G. E. Erickson et al., pp. 59–90, Circum-Pac. Council for Energy and Miner. Resour., Houston, Tex.
- Muñoz, N., and R. Charrier (1996), Uplift of the western border of the Altiplano on a west-vergent thrust system, northern Chile, *J. S. Am. Earth Sci.*, **9**, 171–181.
- Muñoz, N., and P. Sepúlveda (1992), Estructuras compressivas con vergencia al oeste en el borde oriental de la Depresión Central, norte de Chile (19°15′S), *Rev. Geol. Chile*, **19**, 241–247.
- Naranjo, J. A., and R. Paskoff (1985), Evolución cenozoica del piedemonte andino en la Pampa del Tamarugal, norte de Chile (18°–21°S), paper presented at 4th Congreso Geológico Chileno, Dep. de Geociencia, Univ. Católica del Norte, Antofagasta, Chile.
- Ortlieb, L., C. Zazo, J. L. Goy, C. Hillaire-Marcel, B. Ghaleb, and L. Cournoyer (1996), Coastal deformation and sea-level changes in the northern Chile subduction area (23°S) during the last 330 ky, *Quat. Sci. Rev.*, **15**, 819–831.
- Pardo-Casas, F., and P. Molnar (1987), Relative motion of the Nazca (Farallón) and South American plates since Late Cretaceous time, *Tectonics*, **6**, 233–248.
- Parraguez, G. (1998), Sedimentología y geomorfología producto de la tectónica Cenozoica, en la Depresión Central, Pampa de Chaca, I Región Tarapacá, Chile, thesis, Dep. de Geol., Univ. de Chile, Santiago.
- Pinto, L. (1999), Evolución tectónica y geomorfológica Cenozoica del borde occidental del Altiplano y su registro sedimentario entre los 19°08′S–19°27′S (región de Tarapacá, Chile), thesis, Dep. de Geol., Univ. de Chile, Santiago.
- Pinto, L., G. Hérail, and R. Charrier (2004), Sedimentación sintectónica asociada a las estructuras Neógenas en la Precordillera de la zona de Moquella (19°15′S, norte de Chile), *Rev. Geol. Chile*, **31**, 19–44.
- Ramos, V. (1988), The tectonics of the central Andes: 30° to 33°S latitude, in *Processes in Continental Lithospheric Deformation*, edited by S. Clark and D. Burchfiel, *Spec. Pap. Geol. Soc. Am.*, **218**, 31–54.
- Reutter, K.-J., P. Giese, H. J. Götze, E. Scheuber, K. Schwab, G. Schwarz, and P. Wigger (1988), Structure and crustal development of the central Andes between 21° and 25°S, in *The Southern Central Andes*, *Notes Earth Sci.*, vol. 17, edited by H. Bahlburg et al., pp. 231–261, Springer, New York.
- Riba, O. (1976), Syntectonic unconformities of the Alto Cardener, Spanish Pyrenees: A genetic interpretation, *Sediment. Geol.*, **15**, 213–233.
- Riquelme, R. (1998), Evolución tectono-sedimentaria Post-Oligocénica del borde occidental del Altiplano, entre Tignamar y el Salar de Surire, thesis, Dep. de Geol., Univ. de Chile, Santiago.
- Riquelme, R. (2003), Evolution geomorphologique neogene de Andes centrales du Desert d’Atacama (Chili): Interaction tectonique-climat, Ph.D. thesis, Univ. Paul Sabatier, Toulouse, France.
- Riquelme, R., and G. Hérail (1997), Discordancias progresivas en el Cenozoico Superior del borde occidental del Altiplano de Arica: Implicancias en la interpretación tectónica de la Cordillera Occidental, paper presented at 8th Congreso Geológico Chileno, Departamento de Ciencias Geológicas, Univ. Católica del Norte, Antofagasta, Chile.
- Roeder, D. (1988), Andean-age structure of Eastern Cordillera (province of La Paz, Bolivia), *Tectonics*, **7**, 23–39.
- Rutland, R. W. R. (1971), Andean orogeny and sea floor spreading, *Nature*, **233**, 252–255.
- Salas, R., R. Kast, F. Montecinos, and I. Salas (1966), Geología y recursos minerales del Departamento de Arica, Provincia de Tarapacá, *Bol. 21*, 130 pp., Inst. de Invest. Geol., Santiago, Chile.
- Sayés, J. (1978), Cuadrángulo Guaviña, provincia de Iquique, I region, scale 1:50,000, 43 pp., Inst. de Invest. Geológicas, Santiago, Chile.
- Schmitz, M. (1994), A balanced model of the southern central Andes, *Tectonics*, **13**, 484–492.
- Sempere, T., G. Hérail, J. Oller, and M. Bonhomme (1990), Late Oligocene-early Miocene major tectonic crisis and related basins in Bolivia, *Geology*, **18**, 946–949.
- Sheffels, B. (1990), Lower bound on the amount of crustal shortening in the central Bolivian Andes, *Geology*, **18**, 812–815.
- Somoza, R. (1998), Updated Nazca (Farallones)-South America relative motions during the last 40 My: Implications for mountain building in the central Andes region, *J. S. Am. Earth Sci.*, **11**, 211–215.
- Stanistreet, I. G., and T. S. McCarthy (1993), The Okavango Fan and the classification of subaerial fans, *Sediment. Geol.*, **85**, 114–133.
- Tassara, A. (2005), Interaction between the Nazca and South American plates and formation of the Altiplano-Puna plateau: Review of a flexural analysis along the Andean margin (15°–34°S), *Tectonophysics*, **399**, 39–57. (doi:10.1016/j.tecto.2004.12.014)
- Tobar, A., R. Salas, and R. Kast (1968), Cuadrángulos Camaraca y Azapa, Provincia de Tarapacá, *Carta Geol. Chile*, **19–20**, 13 pp.
- Tosdal, R., A. Clark, and E. Farrar (1984), Cenozoic polyphase landscape and tectonic evolution of the Cordillera Occidental, southernmost Peru, *Geol. Soc. Am. Bull.*, **95**, 1318–1332.
- Uhlig, D., H. Seyfried, G. Wörner, I. Kohler, and W. Schröder (1996), Landscape evolution in Northernmost Chile (18.5°–19.5°S): Implications in the tectonic, sedimentary, and magmatic history of the central Andes, paper presented at 3rd International Symposium on Andean Geodynamics, Inst. Fr. de Rech. Sci. pour le Dev. en Coop. (ORSTOM), St. Malo, France.

- Victor, P., O. Oncken, and J. Glodny (2004), Uplift of the western Altiplano plateau: Evidence from the Precordillera between 20° and 21°S (northern Chile), *Tectonics*, 23, TC4004, doi:10.1029/2003TC001519.
- Viteri, E. (1979), Geología y recursos minerales de la Formación Huaylas en el Altiplano de Arica, paper presented at 2nd Congreso Geológico Chileno, Inst. de Invest. Geol. de Chile, Arica.
- Vögel, S., and T. Vila (1980), Cuadrángulos Arica y Poconchile, Región de Tarapaca, *Carta Geol. Chile*, 35, 24 pp.
- Weaver, B. L., and J. Tarney (1984), Empirical approach to estimating the composition of the continental crust, *Nature*, 310, 575–577.
- Whitman, D., B. L. Isacks, and S. M. Kay (1996), Lithospheric structure and along-strike segmentation of the central Andes Plateau: Seismic Q , magmatism, flexure, topography and tectonics, *Tectonophysics*, 259, 29–40.
- Wörner, G., and H. Seyfried (2001), Reply to the comment by M. García and G. Hérail on ‘Geochronology (Ar-Ar, K-Ar and He-exposure ages) of Cenozoic magmatic rocks from northern Chile (18–22°S): Implications for magmatism and tectonic evolution of the central Andes’ of Wörner et al. (2000), *Rev. Geol. Chile*, 28, 131–137.
- Wörner, G., K. Hammerschmidt, F. Henjes-Kunst, J. Lezaun, and H. Wilke (2000), Geochronology ($^{40}\text{Ar}/^{39}\text{Ar}$, K-Ar and He-exposure ages) of Cenozoic magmatic rocks from northern Chile (18–22°S): Implications for magmatism and tectonic evolution of the central Andes, *Rev. Geol. Chile*, 27, 205–240.
- Yuan, X., et al. (2000), Subduction and collision processes in the central Andes constrained by converted seismic phases, *Nature*, 408, 958–961.

R. Charrier and M. Farías, Departamento de Geología, Universidad de Chile, Casilla 13518, Correo 21, Santiago, Chile. (mfarias@dgf.uchile.cl)

D. Comte, Departamento de Geofísica, Universidad de Chile, Casilla 2777, Correo 21, Santiago, Chile.

G. Hérail, Institut de Recherche pour le Développement, LMTG, 14 avenue Edouard Belin, F-31400 Toulouse, France.

J. Martinod, Laboratoire des Mécanismes et Transferts en Géologie, Université Paul Sabatier, 14 avenue Edouard Belin, F-31400 Toulouse, France.

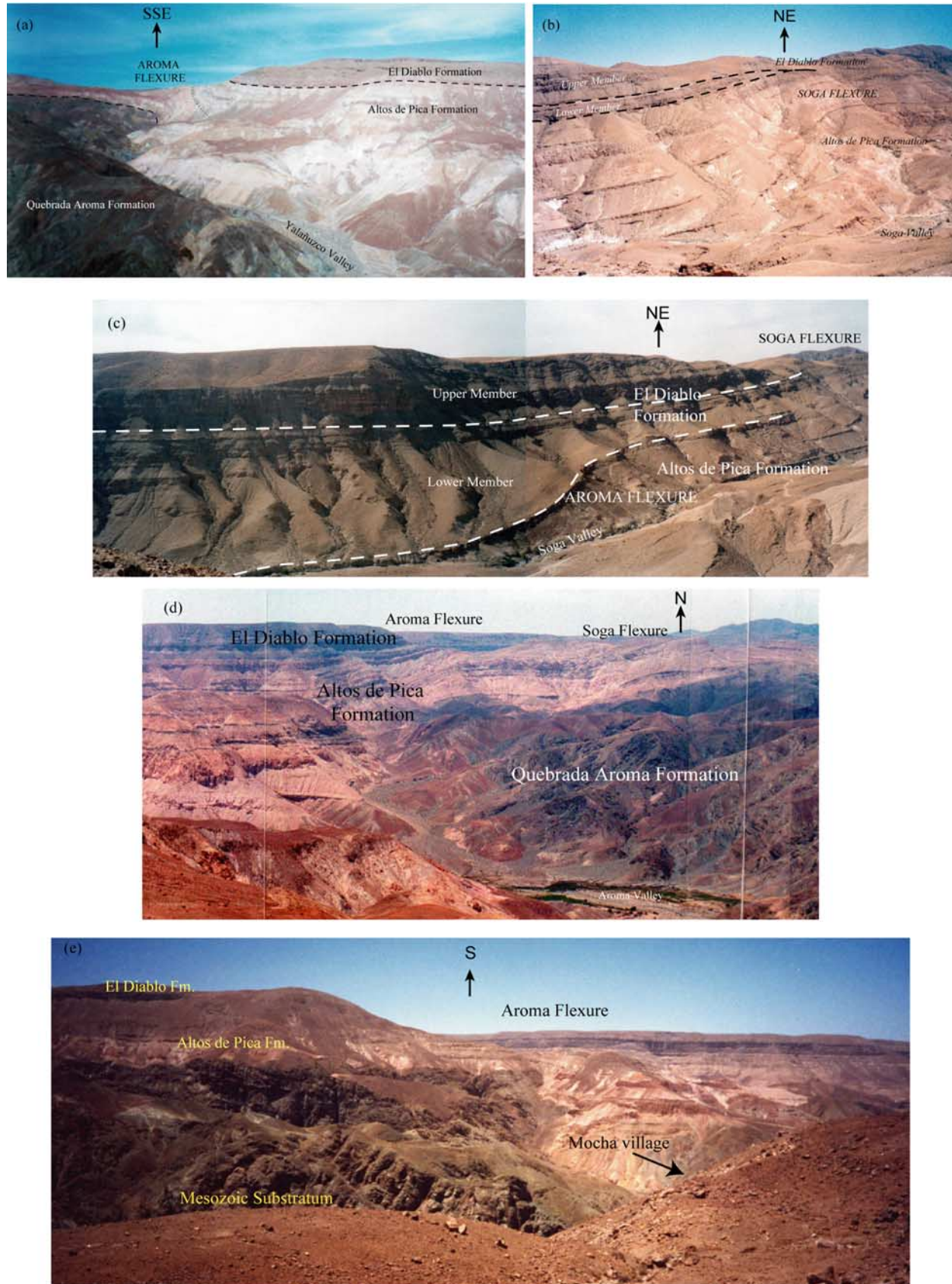


Figure 7

Figure 7. Photographs of the Aroma and Soga flexures. (a) View of the Aroma flexure in the Yalañuzco valley. (b) View of the Soga flexure in the Soga valley. (c) View of Aroma (left) and Soga (right) flexures in the Soga valley. (d). View of both flexures from the headwater of the Yalañuzco valley. (e). View of the Aroma flexure in the Tarapacá valley next to Mocha. Note that the dip of the substratum follows the same style as the deformation of the Cenozoic series.